forests

MDPI

Article

Increased Soil Bacterial Abundance but Decreased Bacterial Diversity and Shifted Bacterial Community Composition Following Secondary Succession of Old-Field

Wen Yang [1,*], Xinwen Cai [1], Yaqi Wang [1], Longfei Diao [1], Lu Xia [2], Shuqing An [2], Yiqi Luo [3] and Xiaoli Cheng [4,*]

[1] College of Life Sciences, Shaanxi Normal University, Xi'an 710119, China
[2] School of Life Sciences, Nanjing University, Nanjing 210023, China
[3] School of Integrative Plant Sciences, Cornell University, Ithaca, NY 14850, USA
[4] School of Ecology and Environmental Sciences, Yunnan University, Kunming 650091, China
* Correspondence: wenyang@snnu.edu.cn (W.Y.); xlcheng@fudan.edu.cn (X.C.); Tel./Fax: +86-29-85310623 (W.Y.); +86-871-65033547 (X.C.)

Abstract: Plant secondary succession is a very effective approach for the rejuvenation of degraded ecosystems. In order to comprehend alterations and driving mechanisms of soil bacterial communities under secondary succession of old-field and reveal their subsequent impacts on the decomposition and accumulation of soil organic carbon (SOC) and nitrogen (SON), we investigated changes in soil bacterial communities following ~160 years of old-field succession on the Loess Plateau of China through analyses of quantitative polymerase chain reaction (qPCR) and Illumina MiSeq DNA sequencing of 16S rRNA genes. Our results revealed that subsequent to secondary succession of old-field, soil bacterial abundance progressively increased, while bacterial richness and diversity significantly decreased. Principal component analysis and Bray–Curtis similarity index showed that bacterial community composition gradually shifted following old-field succession. Specifically, the relative abundances of *Proteobacteria*, *Rokubacteria*, and *Verrucomicrobia* progressively increased, while *Actinobacteria* and *Firmicutes* slightly decreased following old-field succession. The most enriched of *Proteobacteria* (e.g., *Rhizobiales*, *Xanthobacteraceae*, *Gammaproteobacteria*, *Bradyrhizobium*, *Rhizobiaceae*, and *Mesorhizobiur*) were found in a climax forest, while *Chloroflexi* and *Gemmatimonadetes* had the lowest relative abundances. Further, the most enriched members of *Actinobacteria*, including *Geodermatophilaceae*, *Frankiales*, *Blastococcus*, *Micrococcales*, *Micrococcacea*, *Propionibacteriales*, *Nocardioidaceae*, *Nocardioide*, and *Streptomycetaceae*, were exhibited in the farmland stage. Our results suggested that secondary succession of old-field greatly modified soil bacterial communities via the transformation of soil nutrients levels, altering plant biomass and soil physiochemical properties. Soil bacterial community composition was transformed from oligotrophic groups to copiotrophic *Proteobacteria* following old-field succession, which may promote SOC and SON accumulation through increasing the utilization of labile organic carbon (C) and nitrogen (N), while decreasing decomposition of recalcitrant organic C and N from the early- to late-successional stages.

Keywords: 16S rRNA gene; Loess Plateau; bacterial community composition; bacterial diversity; soil nutrient substrates; vegetation restoration

Citation: Yang, W.; Cai, X.; Wang, Y.; Diao, L.; Xia, L.; An, S.; Luo, Y.; Cheng, X. Increased Soil Bacterial Abundance but Decreased Bacterial Diversity and Shifted Bacterial Community Composition Following Secondary Succession of Old-Field. *Forests* **2022**, *13*, 1628. https://doi.org/10.3390/f13101628

Academic Editor: Josu G. Alday

Received: 1 July 2022
Accepted: 28 September 2022
Published: 4 October 2022

1. Introduction

The abandonment of farmlands is a global issue that has been influencing all parts of the world for decades [1,2]. Campbell et al. (2008) reported that the total abandoned farmlands (i.e., old-field) area ranges between 3.85 and 4.72 million km^2 [1,3]. Old-fields are important sites for plant secondary succession [4]. Secondary succession of old-field without further anthropogenic interference is an effective strategy that has positive impacts on the restoration of degraded ecosystems [5], through the enhancement of net primary productivity and recuperation of soil nutrients [6], decreased soil erodibility [7],

and reestablishment of associated ecosystem services [8]. During the process of secondary succession, the composition of plant species, species richness, and plant coverage can be profoundly modified [9,10]. Further, these changes drive alterations in soil physicochemical properties, biogeochemical cycling (e.g., carbon (C), nitrogen (N)) [6,11], and soil microbial characteristics [9,11]. Secondary succession of old-field essentially involves interactions between aboveground vegetation communities and belowground soil microbes [12]. Soil microbes are essential to maintain the stability of belowground ecosystem structure and function [13]. Bacteria comprise over 90% of all soil microbial communities [14] and are well-acknowledged as the most enriched and diverse groups in microbes [15]. Soil bacteria are considered as important driving forces in the regulation of C and N biogeochemical cycling, and the decomposition of litter and soil organic matter (SOM) in terrestrial ecosystems [15,16], as they secrete various extracellular enzymes to decompose litter and organic matter (OM), as well as to convert organic debris into smaller soluble molecules for microbial assimilation [17]. Additionally, soil bacteria actively participate in the formation and transformation of humus [18], promoting edaphic conditions as well as plant establishment after land-use changes [19,20]. Hence, a comprehensive assessment of the variations in soil bacterial communities following old-field succession is helpful toward revealing the mechanisms that drive belowground biogeochemical cycling during old-field succession. Further, it is helpful for detecting the soil quality restoration status and providing useful information for the sustainable restoration of degraded ecosystems.

The responses of soil bacterial communities to old-field succession have attracted increased attention [9–11]. Previous studies reported that secondary succession of old-field progressively enhanced the bacterial richness and diversity of soil over ~30 years of spontaneous succession in abandoned farmland [21]. In contrast, several studies revealed that secondary succession of old-field resulted in the decreased diversity of soil bacteria [22,23]. For instance, Wang et al. (2021) revealed that bacterial diversity was greatest in farmland, which continuously declined along with ~40 years of secondary succession in a karst area [23]. Zhong et al. (2020) documented that although the diversity and evenness of vegetation communities were enhanced, soil bacterial diversity initially increased, reaching a maximum at 30 years, which then decreased following ~50 years of secondary succession [22]. These inconsistent results might be attributed to variations in the duration of secondary succession, vegetation types, heterogeneity of ecosystems, previous land use histories, and soil microclimates [24]. Thus, an identification of the alterations and driving mechanisms of soil bacterial communities following long-term old-field succession is urgently required.

Soil bacterial communities are dynamic integrations of various driving forces, including biotic (e.g., vegetation type and diversity, plant litter, and root exudates) [25,26] and abiotic factors, such as soil nutrient substrates [27,28], soil moisture [29,30], pH [31], and climate [32]. Shifts in plant compositions, diversity, and canopy density can modify abiotic soil properties (e.g., moisture, pH, nutrient substrates levels) through changing quantity and quality of plant residues that enter soil, which eventually impact on abundance, diversity, and community composition for soil bacterial communities [19,23,33]. Soil nutrient substrates have been confirmed to be the vital driving factor for soil bacterial communities as they are dependent on the decomposition of nutrient substrates to obtain energy [27,28]. However, responses of distinct taxa of bacterial communities to nutrient availability are diverse [34]. For instance, *Actinobacteria*, *Chloroflexi*, *Gemmatimonadetes*, and *Cyanobacteria* flourish in nutrient-deprived environments, preferring to use recalcitrant C substrates [35,36]. Conversely, *Proteobacteria* thrive in nutrient-rich environments with sufficient labile C substrates [37,38]. Additionally, soil moisture is a vital factor that mediates bacterial abundance, structure through affecting physiological activities of bacteria, and the availability and transport of oxygen and nutrients [29,39]. Soil pH is of paramount importance for driving soil bacterial community [2,31,40], owing to different soil pH levels that affect the adaptation and selection of particular bacterial community taxa. Identifying the factors which drive changes in soil bacterial abundance, diversity, and community

composition following secondary succession in degraded ecosystems can be instrumental toward a comprehensive understanding of the influencing mechanisms of old-field succession on soil bacterial communities.

The Loess Plateau of China (LPC) inhabits the middle and upper reaches of the Yellow River with an area of 624,000 km^2 and has been considered as one of the most ecologically fragile areas in the world, due to severe soil erosion and frequent anthropogenic disturbances [41]. In an attempt to recover these fragile ecosystems, a variety of restoration strategies have been implemented since the 1950s. The most important endeavor was the implementation of the largest ecological engineering "Grain for Green" program in China in 1999 [41,42], which involved the conversion of croplands at inclines of more than 15° to grassland, shrubland, or forest through secondary succession or afforestation [42]. Previous studies revealed that secondary succession of old-field greatly decreased soil erosion [7], modified the properties of plants and soil [43], as well as the accumulation and stabilization of soil organic C and N on the LPC [43,44]. Further reports quantified the responses of soil microbial or bacterial communities to afforestation [45], and/or secondary succession of old-field in the short-term (less than 60 years) [21–23]. However, the impacts of long-term old-field succession on soil bacterial abundance, diversity, and community composition following a chronosequence have received little attention. In this study, we hypothesize that: (i) long-term old-field succession significantly increases soil bacterial abundance which is largely due to the increase in soil nutrient substrates levels and soil moisture; (ii) long-term old-field succession decreases soil bacterial diversity during old-field succession; (iii) the composition of soil bacterial communities is transformed from oligotrophic groups to copiotrophic groups following old-field succession, which is primarily driven by variations in soil nutrient substrates, plant and physicochemical properties, and light intensity. To test these hypotheses, Illumina MiSeq sequencing of bacterial 16S rRNA genes and quantitative polymerase chain reactions (qPCR) was performed. This was done to analyze variations in the soil bacterial abundance, diversity, and community composition following long-term old-field succession, which spanned a ~160 year period from farmland to climax forest on the LPC. Twelve environmental variables were examined to identify the primary factors that drove soil bacterial communities.

2. Materials and Methods

2.1. Study Site

This study was conducted on the northwest side of the Ziwuling Mountains, in the central region of the LPC (36°00′14″–36°01′09″ N and 109°00′56″–109°01′52″ E), Fu County, Shaanxi Province, China (Figure 1a,b). This area has a mean annual temperature and rainfall of 9 °C and 576.7 mm, respectively, and is home to typical hilly and gullied landscapes with elevations that span from 1157−1369 m [5]. This region of the LPC was subjected to suffering the most serious soil erosion. Secondary succession of old-field in conjunction with continued deforestation in Ziwuling Forest caused the emergence of secondary forest that spanned approximately 23,000 km^2. Secondary succession has naturally regenerated on old-field (*Zea mays* Linnaeus was the main original rotation crop prior to secondary succession), according to previous research in the study area. Since 1860, the abandonment of this land occurred a number of times when the local population was displaced due to war, food scarcity, and other calamities. Consequently, various stages of secondary succession, from pioneer weeds and herbage, to shrubland, and to early and climax forests (*Quercus mongolica* Fischer ex Ledebour), have been observed in this area over the last ~160 years [46]. Chen et al. (1954) revealed that *Populus davidiana* Dode was the dominant species in this region following ~100 years of secondary succession [47]. The prolonged existence of pioneer weeds, herbage, and shrub was determined through discussions with local elders, and by investigating land agreements between farmers and the government.

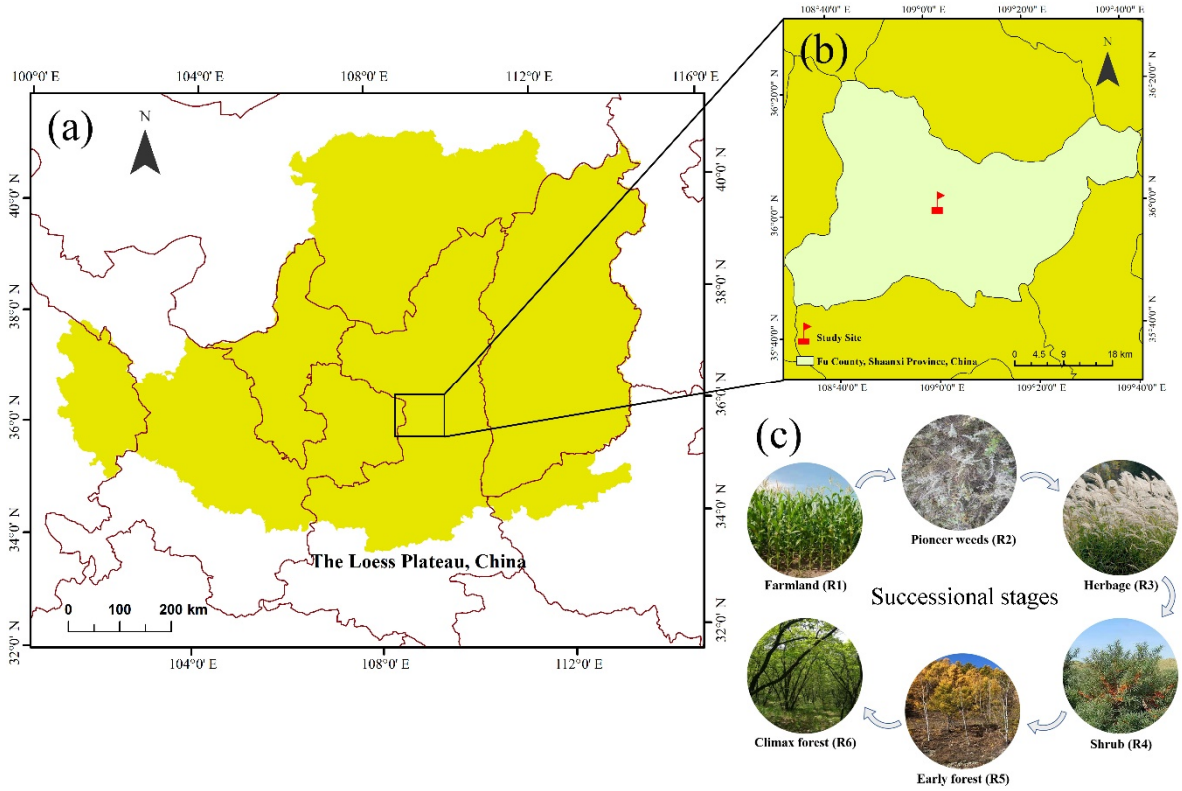

Figure 1. (**a**) The geographical location of the Loess Plateau, China, (**b**) the study site in Fu County, Shaanxi Province, China, (**c**) and the photographs of the study site at each successional stage.

The investigation of old-field succession for this study was implemented in October 2019. Six typical secondary successional stages (R1–R6) were selected as samples for this study: (1) farmland stage (the control, 0 year, R1), in which *Zea mays* Linnaeus was the main rotation crop prior to succession; (2) pioneer weeds stage (~15 years, R2), which was dominated by *Artemisia lavandulifolia* Candolle and *Stipa bungeana* Trinius communities; (3) herbage stage (~30 years, R3), in which *Miscanthus sacchariflorus*(Maximowicz) Hackel communities were the main dominant herbaceous species; (4) shrub stage (~50 years, R4), which was dominated by *Hippophae rhamnoides* Linnaeus communities; (5) early forest stage (~110 years, R5), which was dominated by *P. davidiana* communities; and (6) climax forest stage (~160 years, R6), which was dominated by *Q. mongolica* communities (Figure 1c). These secondary successional stages did not suffer from natural (e.g., wildfire) or human disturbance, except for the farmland stage during the process of old-field succession through field investigation and consultations with local elders and administrators of forestry stations.

2.2. Soil and Plant Sampling

Soil and plant samples were collected in October 2019, and four replicate plots were randomly established in each successional stage. The sampling plot dimensions were 2 m × 2 m in the farmland, pioneer weeds, and herbage communities, 5 m × 5 m in the shrub community, and 20 m × 20 m in the early and climax forests, respectively. The distances between adjacent plots in each successional stage were 200 m at minimum, but not greater than 2 km at elevations lower than 120 m. All plots for each successional stage had similar slope gradients and slope aspects to ensure consistent environmental conditions. Before soil sampling, geographical features and vegetation information of each successional stage were investigated and are shown in Table S1. Three 1 m × 1 m quadrats were randomly established in each plot for the early and climax forests, and shrub communities, respectively, to record the name, number, density, coverage, and frequency of each species. All the name, number, density, coverage, and frequency of each species were

recorded in each of sampling plot (2 m × 2 m) for the farmland, pioneer weeds, and herbage communities, respectively. Plant species richness is the total number of species in each plot [48]. Plant species diversity and evenness were calculated using the Shannon-Wiener Diversity Index and Pielou Evenness Index, respectively [48]. After recording, all litter in each quadrat were gathered, and three root sampling blocks (10 cm diameter) from each plot were collected to obtain belowground roots at the 0–20 cm soil layer. A total of 72 litter and 72 root samples were obtained. The S-shaped sampling technique was employed to randomly extract nine soil samples (Ø5 cm × 20 cm deep) from each plot. The soil samples of every plot were completely mixed to produce a single composite for a total of 24 soil samples (six successional stages × four replicates). All soil samples were sifted through a 2 mm sieve to eliminate visible roots and debris and then mixed thoroughly. A portion of each soil sample was collected in a 50 mL centrifuge tube and frozen, which was then placed in a dry-ice box and transferred to the laboratory with all of the soil and plant samples.

2.3. Analysis of Soil and Plant Properties

In the laboratory, soil samples in the tubes were immediately stored at −80 °C for DNA extraction. The remaining soil samples were segregated as four subsamples after thorough mixing. To quantify the soil moisture, the first subsample was dried at 105 °C to a constant weight. To assess the soil pH, soil organic carbon (SOC), and soil organic nitrogen (SON), the second subsample was dried in ambient air and passed through a 1 mm sieve. The third soil subsample was air-dried and passed through a 0.15 mm sieve to determine total nitrogen (TN), ammonium nitrogen (NH_4^+-N), nitrate nitrogen (NO_3^--N), total phosphorus (TP), and available phosphorus (AP). The fourth fresh soil subsample was stored at 4 °C to determine water-soluble organic C (WSOC). Each root sample block was continuously rinsed with water using a 0.15 mm sieve, after which the remaining roots were collected. All of the litter and root samples were cleaned and dried at 65 °C to a constant weight to measure litter and root biomass, respectively. Soil pH value was measured using a pH meter at a soil/water ratio of 1:2.5. SOC and SON concentrations were quantified using a Vario PYRO cube elemental analyzer (Elementar Analysensysteme GmbH, Hanau, Germany). Prior to the measurements, the air-dried soil samples were treated with 1 M HCl for 24 h at room temperature in to eliminate all carbonates. WSOC concentration was determined using a Liqui TOCII analyzer (Elementar Analysensysteme GmbH, Hanau, Germany) using the technique described by Yang et al. (2016) [49]. TN concentration was measured using an AA3 continuous flow analyzer (SEAL Analytical GmbH, Norderstedt, Germany) subsequent to digestion with H_2SO_4 and extraction with 1M KCl. TP and AP concentrations were determined using the molybdophosphate method, which digested the soil with a mixture of $HClO_4$ and H_2SO_4 before measuring with an AA3 continuous flow analyzer. NH_4^+-N and NO_3^--N concentrations were measured using an AA3 continuous flow analyzer after the samples were extracted with 1 M KCl.

2.4. Soil DNA Extraction and q-PCR

A Power Soil DNA kit (MoBio Laboratories, Carlsbad, CA, USA) was employed, in accordance with manufacturer's protocol, to extract soil microbial DNA from frozen soil samples (equivalent to 0.5 g dry weight). Extracted soil microbial DNA was divided into two parts. The first microbial DNA subsample was utilized for qPCR analysis, whereas the second microbial DNA subsample was employed for Illumina MiSeq sequencing. Soil bacterial abundance was quantified via qPCR analysis of the V3–V4 regions of bacterial 16S rRNA gene with the 338F primer (5′-ACTCCTACGGGAGGCAGCA-3′) and 806R primer (5′-GGACTACHVGGGTWTCTAAT-3′) [40]. The reaction volume was 25 µL, and was comprised of SYBR Green qPCR Master Mix (2×) (Applied Biosystems, Foster City, CA, USA) (12.5 µL), template DNA (diluted five times) (2 µL), forward and reverse primers (0.5 µL of 10 µM), and ddH_2O (9.5 µL). The 16S rRNA gene was amplified using an ABI 7500 real-time PCR system (Applied Biosystems, Foster City, CA, USA). The cycling conditions

were as follows: 10 min at 95 °C, 40 cycles of 15 s at 95 °C, and 1 min at 60 °C. All real-time PCR reactions on the DNA extracted from each soil sample were run in triplicate. The 16S rRNA copy number was calculated using the formula described by Sun et al. (2015) [50].

2.5. PCR Amplification and Illumina MiSeq Sequencing

The 338F primer (5′-ACTCCTACGGGAGGCAGCA-3′) and 806R primer (5′-GGACTACHVGGGTWTCTAAT-3′) were designed to amplify the V3–V4 regions of the bacterial 16S rRNA gene. The bacterial amplification PCR reaction mixture was used in triplicate, with each containing 4 µL of 5 × FastPfu buffer, 2 µL of 2.5 mM deoxynucleotide triphosphates (dNTPs), 0.8 µL forward primer (5 µM), 0.8 µL reverse primer (5 µM), 0.4 µL of FastPfu Polymerase, 0.2 µL of BSA, 10 ng of Template DNA, and ddH_2O added to a final volume of 20 µL. The PCR reaction was performed with an initial denaturation step at 95 °C for 3 min, followed by 27 cycles of 95 °C for 30 s, 55 °C for 30 s, and 72 °C for 45 s, 72 °C for 10 min, and 10 °C until halted by the user. The PCR reactions were conducted with an ABI GeneAmp® 9700 PCR System (Applied Biosystems, Foster City, CA, USA). Successful PCR amplifications were extracted from 2% agarose gels, purified using the AxyPrep DNA Gel Extraction Kit (Axygen Biosciences, Union City, CA, USA), and quantified with the QuantiFluor-ST blue fluorescence quantitative system (Promega, Madison, WI, USA). The purified amplicons were pooled in equimolar ratios and subjected to paired-end sequencing (2 × 300) on an Illumina MiSeq PE300 platform (Illumina Corporation, San Diego, CA, USA) from Majorbio Biopharm Technology Co., Ltd, Shanghai, China.

2.6. Sequencing Data Processing

The software package, Quantitative Insights into Microbial Ecology (QIIME; v. 1.9.1, http://qiime.org/install/index.html, accessed on 10 May 2020) [51], was employed to process the sequences derived from the Illumina MiSeq platform. Subsequently, employing the standards articulated below, the unprocessed FASTQ files were demultiplexed, quality-filtered using Trimmomatic v. 0.32 [52], and then merged using FLASH (v. 1.2.11, https://ccb.jhu.edu/software/FLASH/index.shtml, accessed on 13 May 2020): (a) Low quality sequence read segments, with typical quality values of <20 over a 50 bp sliding window, as well as those sequences that included >6 bp homopolymeric segments, were deleted from paired-end sequence read files [52]. (b) The closely matched primers allowed for only two nucleotide sequence mismatches, whereas those reads that had equivocal bases were rejected. (c) Sequences containing >10 bp overlaps were joined contingently on their overlap sequence. Using Illumina MiSeq sequencing, 1,278,288 reads overall were extracted from the 24 soil samples. A similar level of sequencing penetration for later analyses was acquired by randomly selecting the minimum number of reads (i.e., 40,838) in all of the subsets from each sample with the Mothur program (v. 1.30.2, https://www.mothur.org/wiki/Download_mothur, accessed on 15 May 2020), which finally generated 980,112 reads from 24 soil samples. Next, subsampled sequences were categorized according to their operational taxonomic units (OTUs), at similarity levels of 97% utilizing the UPARSE method (v. 7.0.1090, http://www.drive5.com/uparse/, accessed on 15 May 2020) [53]. To compare bacterial richness and diversity subsequent to the acquisition of 69,659 OTUs (in total) from the 24 soil samples, the Mothur program (v. 1.30.2) [54] was employed to calculate the OTU richness (total population of quantified OTUs), Chao's species richness estimation (Chao1), abundance-based coverage estimation (ACE), Shannon diversity indices, OTUs rarefaction curves, and Shannon-Wiener curves. Taxonomic phylum, class, order, family, and genus categorizations were designated using a Ribosomal Database Project (RDP) Bayesian classifier (v. 11.5, http://rdp.cme.msu.edu/, accessed on 25 May 2020). Next, tags were contrasted against the bacterial 16S rRNA Silva reference database (v. 138, https://www.arb-silva.de/, accessed on 25 May 2020) to identify chimeric sequences [55]. To identify any possible statistically meaningful taxa from the soil bacterial communities between the various treatments, linear discriminant analysis (LDA) effect size (LEfSe) was engaged. A cladogram was developed with LEfSe (R software v. 3.2.2.),

which elucidated phylogenetic distribution of microbial lineages that were correlated with six defined successional stages, having LDA values of 3.5 or higher. Finally, the complete dataset was deposited into the Sequence Read Archive (SRA) database of the National Center for Biotechnology Information (NCBI) (https://www.ncbi.nlm.nih.gov/, accessed on 16 August 2022) under the accession number of SRP392368.

2.7. Statistical Analysis

One-way ANOVA was used to assess the impacts of old-field succession on plant and soil properties and soil bacterial communities. Significant variations between the means of the groups were evaluated with Duncan's test at $p < 0.05$. Principal component analysis (PCA) of the OTUs data was completed using R software v. 3.2.2, whereas the Bray–Curtis similarity index was determined via the OTU reads. A beta-diversity distance matrix was employed to determine the hierarchical clustering with QIIME software package v. 1.9.1. Redundancy analysis (RDA) was employed to investigate the relationships between soil bacterial community composition at the phylum- and class-level with properties of plant (i.e., LB and RB) and soil properties (i.e., soil moisture, TP, NO_3^--N, WSOC, SON, pH, NH_4^+-N, AP, TN, and SOC) using CANOCO 4.5 software. The statistical significance of the RDA was tested using Monte Carlo permutation tests (499 permutations; $p < 0.05$) in the CANOCO 4.5 software. Pearson's correlation analysis was employed to evaluate the relationships of soil bacterial abundance (i.e., gene of 16S rRNA copies), bacterial richness (i.e., ACE and Chao1), diversity (i.e., Shannon), and the relative abundances of the dominant bacterial phyla and classes, with plant and soil properties, respectively.

3. Results

3.1. Variations in Plant and Soil Characteristics Following Old-Field Succession

Plant species richness was highest in the early forest, followed by climax forest, pioneer weeds, herbage, and shrub stages, and was lowest in the farmland (Table S1). Plant species diversity and evenness were highest in the early forest and the shrub stage, respectively (Table S1). Litter and root biomass, soil pH, moisture, SOC, WSOC, TN, SON, NO_3^--N, and AP were significantly affected by old-field succession (Table S2). Litter biomass increased substantially from 25 to 956 g m^{-2} following old-field succession (Table S2). The climax forest, early forest, and farmland stages exhibited greater root biomass in contrast to pioneer weeds, herbage, and shrub stages (Table S2). Soil pH was highest in the farmland, pioneer weeds, and herbage stages between successional stages (Table S2). Soil moisture, SOC, WSOC, TN, and SON concentrations continuously increased following old-field succession (Table S2). Soil NH_4^+-N concentration was lowest in the farmland (Table S2). Soil NO_3^--N concentration in the farmland and shrub stages were considerably higher than that in the pioneer weeds, herbage, early, and climax forest stages (Table S2). Soil TP concentration was virtually unchanged following old-field succession (Table S2), whereas soil AP concentration was greatest in the farmland stage between successional stages (Table S2).

3.2. Variations in the Abundance and Alpha-Diversity of Soil Bacterial Communities Following Old-Field Succession

The total bacterial abundance was 2.33×10^9 copies/g in the farmland stage, 3.05×10^9 copies/g in the pioneer weeds stage, 3.51×10^9 copies/g in the herbage stage, 4.01×10^9 copies/g in the shrub stage, 4.63×10^9 copies/g in the early forest stage, and 5.67×10^9 copies/g in the climax forest stage (Figure 2). Total bacterial abundance gradually increased following old-field succession, achieving its maximum in the climax forest (Figure 2).

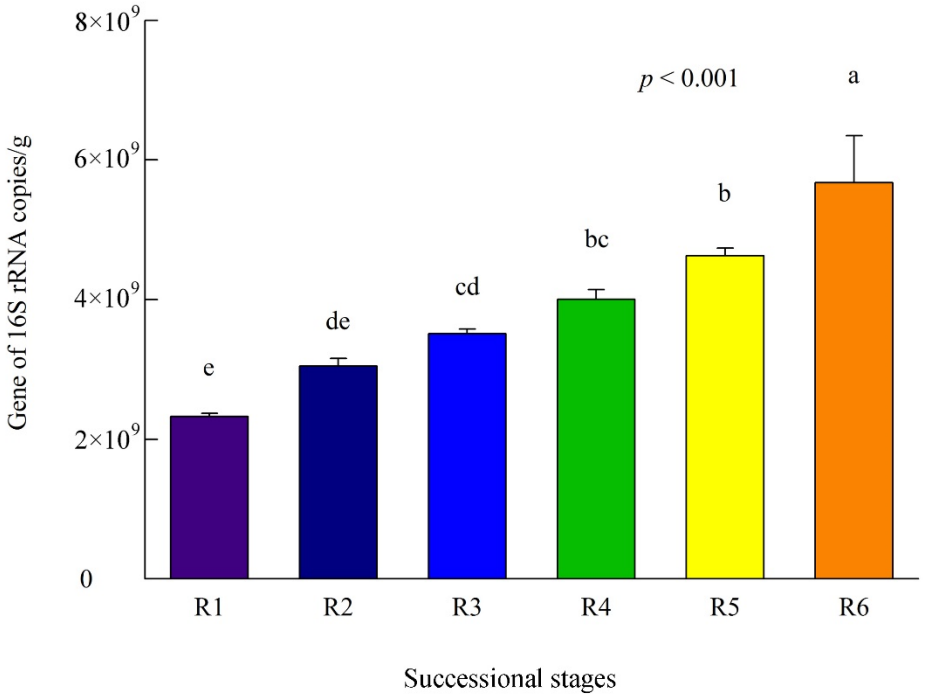

Figure 2. Total bacterial abundance was indicated by the 16S rRNA copies per gram of soil (mean ± SE, n = 4) (0–20 cm depth) of different successional stages on the Loess Plateau of China. Different lower-case letters indicate statistically significant differences at the α = 0.05 level between successional stages. R1: Farmland control; R2: Pioneer weeds; R3: Herbage (*M. sacchariflorus*); R4: Shrub (*H. rhamnoides*); R5: Early forest (*P. davidiana*); and R6: Climax forest (*Q. mongolica*).

The bacterial OTU richness was greatest in the farmland stage (Table 1). Species richness indices (i.e., Chao1 and ACE) for soil bacterial communities in the climax forest were markedly lower than those for other successional stages (Table 1). Similarly, climax forest exhibited a flatter rarefaction curve with the lowest taxon richness relative to other successional stages (Figure S1a). The Shannon diversity index for soil bacterial communities in farmland, pioneer weeds, herbage, and shrubs was considerably higher than that in climax forest (Table 1). Shannon curve flattened out at reads below 5000 for each soil sample and showed that the climax forest soil had the lowest bacterial diversity (Figure S1b). The coverage of soil samples ranged from 97.60% to 98.00% between successional stages (Table 1).

Table 1. Number of sequences analyzed and observed soil bacterial community richness and diversity indices (mean ± SE, n = 4) at different successional stages on the Loess Plateau of China, obtained for clustering at 97% identity.

Characteristics	Successional Stages						Source of Variation
	Farmland (R1)	Pioneer Weeds (R2)	Herbage (R3)	Shrub (R4)	Early Forest (R5)	Climax Forest (R6)	
Reads	40,838	40,838	40,838	40,838	40,838	40,838	-
OTU richness	3113 ± 77 ^{a}	2946 ± 42 ^{ab}	2977 ± 130 ^{ab}	2881 ± 89 ^{abc}	2901 ± 68 ^{abc}	2597 ± 41 ^{c}	*
Richness (Chao1)	4038 ± 79 ^{a}	4047 ± 73 ^{a}	3993 ± 142 ^{a}	3979 ± 91 ^{a}	3983 ± 85 ^{a}	3495 ± 70 ^{b}	**
Richness (ACE)	4033 ± 100 ^{a}	4046 ± 57 ^{a}	4004 ± 141 ^{a}	4015 ± 98 ^{a}	3994 ± 82 ^{a}	3477 ± 55 ^{b}	**
Diversity (Shannon)	6.63 ± 0.04 ^{a}	6.59 ± 0.02 ^{a}	6.60 ± 0.08 ^{a}	6.65 ± 0.05 ^{a}	6.55 ± 0.05 ^{ab}	6.41 ± 0.04 ^{b}	*
Coverage (%)	0.9770 ± 0.0005 ^{b}	0.9760 ± 0.0004 ^{b}	0.9766 ± 0.0008 ^{b}	0.9768 ± 0.0006 ^{b}	0.9762 ± 0.0004 ^{b}	0.9800 ± 0.0004 ^{a}	***

* p < 0.05; ** p < 0.01; *** p < 0.001. Different superscript lower case letters indicate statistically significant differences at the α = 0.05 level between successional stages. Reads are the high-quality sequences following filtering and normalization. The richness estimators, diversity indices, and coverage were calculated using the Mothur program. OTU richness: the total number of measured operational taxonomic units (OTUs).

3.3. Variations in the Composition of Soil Bacterial Communities Following Old-Field Succession

The dominant phyla of the soil bacterial communities across all successional stages were *Actinobacteria* (30.77%–39.42%), *Proteobacteria* (22.28%–30.83%), followed by *Acidobacteria* (11.90%–18.13%), and *Chloroflexi* (9.36%–13.68%) (Figure 3). The minor phyla included *Gemmatimonadetes* (2.03%–3.96%), *Rokubacteria* (1.65%–2.61%), *Bacteroidetes* (1.13%–1.72%), *Firmicutes* (0.74%–1.50%), *Planctomycetes* (0.82%–1.58%), *Verrucomicrobia* (0.39%–1.67%), and *Cyanobacteria* (0.03%–0.61%) (Figure 3). *Actinobacteria* was the most dominant bacterial phylum across all successional stages (Figure 3), where the relative abundances of *Actinobacteria* and *Cyanobacteria* were most enriched in the farmland stage (Figure 3). The relative abundance of *Proteobacteria* in the late successional stages (i.e., climax forest and early forest) was considerably higher than that in the early successional stages (Figure 3). Climax forest exhibited the lowest relative abundances of *Chloroflexi* and *Gemmatimonadetes* between successional stages (Figure 3). The relative abundance of *Firmicutes* was most enriched in the farmland and pioneer weeds stages (Figure 3). The relative abundance of *Verrucomicrobia* in the climax forest was obviously higher than that in other successional stages (Figure 3).

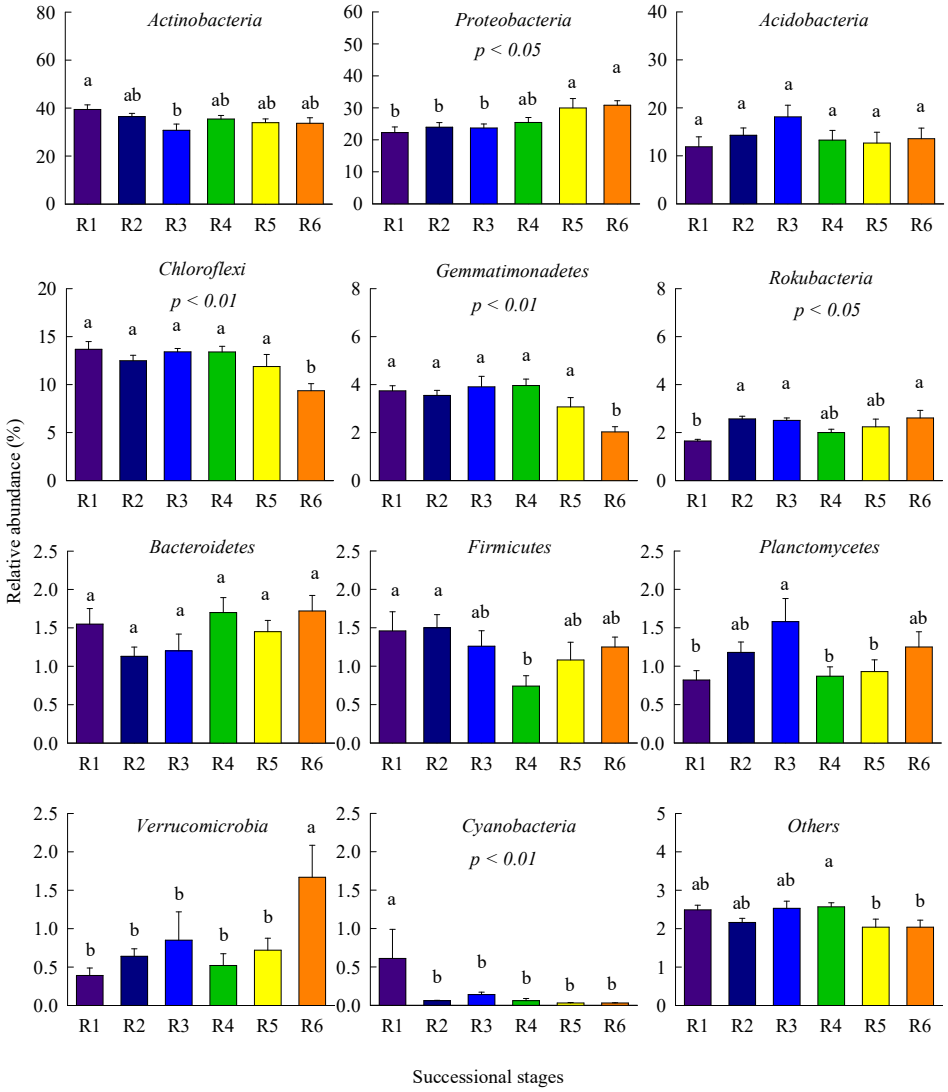

Figure 3. Relative abundance (% of individual taxonomic groups) of the dominant bacterial phyla (mean ± SE, n = 4) present in the microbial communities of different successional stages on the Loess Plateau of China. Different lower-case letters indicate statistically significant differences at the α = 0.05 level between successional stages. See Figure 2 for abbreviations.

At the class level, high levels of bacteria belong to *Actinobacteria*, *Alphaproteobacteria*, *Gammaproteobacteria*, *Deltaproteobacteria*, *Chloroflexia*, and *Gemmatimonadetes* across all soil samples (Table 2). The relative abundances of *Actinobacteria*, *Chloroflexia*, and *Oxyphotobacteria* were most abundant in the farmland stage. The relative abundance of *Alphaproteobacteria* in the early and climax forests was markedly higher than that in other successional stages. The relative abundance of *Gammaproteobacteria* steadily increased following old-field succession. The relative abundance of *Gemmatimonadetes* in the climax forest was markedly lower than that in other successional stages. The relative abundances of *Verrucomicrobiae* and *Acidobacteriia* were considerably higher than that in other successional stages. The relative abundances of *Deltaproteobacteria*, *Bacteroidia*, and *Anaerolineae* showed no obvious changes following old-field succession (Table 2).

Table 2. Relative abundance (% of individual taxonomic groups) of the dominant bacterial classes (mean ± SE, $n = 4$) present in the soil (0–20 cm depth) microbial communities of different successional stages on the Loess Plateau of China.

Class	Successional Stages						Source of Variation
	Farmland (R1)	Pioneer Weeds (R2)	Herbage (R3)	Shrub (R4)	Early Forest (R5)	Climax Forest (R6)	
Actinobacteria	39.42 ± 1.94 ^{a}	36.46 ± 1.33 ^{ab}	30.77 ± 2.58 ^{b}	35.45 ± 1.48 ^{ab}	33.92 ± 1.58 ^{ab}	33.65 ± 2.34 ^{ab}	n.s.
Alphaproteobacteria	14.30 ± 1.19 ^{b}	14.66 ± 0.82 ^{b}	14.13 ± 0.82 ^{b}	15.13 ± 1.02 ^{b}	20.06 ± 2.03 ^{a}	19.58 ± 1.23 ^{a}	**
Gammaproteobacteria	4.77 ± 0.39 ^{d}	5.49 ± 0.43 ^{cd}	5.81 ± 0.43 ^{bcd}	7.12 ± 0.50 ^{ab}	6.83 ± 0.59 ^{abc}	7.89 ± 0.52 ^{a}	**
Deltaproteobacteria	3.20 ± 0.21 ^{a}	3.82 ± 0.33 ^{a}	3.79 ± 0.18 ^{a}	3.19 ± 0.27 ^{a}	3.08 ± 0.37 ^{a}	3.36 ± 0.33 ^{a}	n.s.
Chloroflexia	4.74 ± 0.12 ^{a}	3.56 ± 0.16 ^{bc}	3.99 ± 0.26 ^{b}	3.89 ± 0.46 ^{b}	2.97 ± 0.12 ^{c}	1.78 ± 0.06 ^{d}	n.s.
Gemmatimonadetes	3.74 ± 0.21 ^{a}	3.55 ± 0.21 ^{a}	3.91 ± 0.44 ^{a}	3.96 ± 0.27 ^{a}	3.07 ± 0.39 ^{a}	2.03 ± 0.21 ^{b}	**
Bacteroidia	1.48 ± 0.19 ^{a}	1.10 ± 0.12 ^{a}	1.17 ± 0.21 ^{a}	1.65 ± 0.19 ^{a}	1.42 ± 0.15 ^{a}	1.69 ± 0.20 ^{a}	n.s.
Dehalococcoidia	1.03 ± 0.05 ^{cd}	1.33 ± 0.04 ^{bc}	1.47 ± 0.09 ^{ab}	1.74 ± 0.19 ^{a}	1.00 ± 0.09 ^{d}	1.17 ± 0.06 ^{bcd}	**
Bacilli	1.40 ± 0.25 ^{a}	1.48 ± 0.17 ^{a}	1.24 ± 0.20 ^{ab}	0.73 ± 0.13 ^{b}	1.06 ± 0.23 ^{ab}	1.24 ± 0.13 ^{ab}	n.s.
Anaerolineae	1.33 ± 0.16 ^{a}	1.01 ± 0.05 ^{a}	1.19 ± 0.25 ^{a}	1.25 ± 0.11 ^{a}	1.05 ± 0.17 ^{a}	0.95 ± 0.10 ^{a}	n.s.
Verrucomicrobiae	0.39 ± 0.10 ^{b}	0.64 ± 0.10 ^{b}	0.85 ± 0.37 ^{b}	0.52 ± 0.15 ^{b}	0.72 ± 0.16 ^{b}	1.67 ± 0.42 ^{a}	n.s.
Planctomycetacia	0.38 ± 0.08 ^{b}	0.74 ± 0.12 ^{ab}	1.01 ± 0.26 ^{a}	0.40 ± 0.08 ^{b}	0.50 ± 0.13 ^{b}	0.71 ± 0.13 ^{ab}	n.s.
Acidobacteriia	0.60 ± 0.02 ^{b}	0.42 ± 0.03 ^{b}	0.54 ± 0.05 ^{b}	0.43 ± 0.06 ^{b}	0.42 ± 0.03 ^{b}	1.19 ± 0.17 ^{a}	**
Oxyphotobacteria	0.54 ± 0.38 ^{a}	0.03 ± 0.01 ^{b}	0.11 ± 0.03 ^{ab}	0.04 ± 0.03 ^{b}	0.00 ± 0.00 ^{b}	0.00 ± 0.00 ^{b}	**

** $p < 0.01$; n.s.: not significant. Different superscript lower case letters indicate statistically significant differences at the $\alpha = 0.05$ level between successional stages.

At the order level, the relative abundance of *Rhizobiales* in the early and climax forests was considerably higher than that in other successional stages (Table S3). The relative abundance of *Betaproteobacteriales* was greatest in the climax forest and shrub stages, followed by the early forest, herbage, and pioneer weeds, and was the lowest in the farmland stage. The relative abundance of *Gemmatimonadales* in the climax forest was significantly lower than that in other successional stages. The relative abundances of *Thermomicrobiales*, *Myxococcales*, and *Rubrobacterales* gradually declined following old-field succession. The relative abundances of *Micrococcales* and *Frankiales* were greatest in the farmland stage, followed by the shrub, early forest, herbage, and pioneer weeds stages, and was lowest in the climax forest. The relative abundances of *Myxococcales* and *Rubrobacterales* continually decreased following old-field succession. The relative abundances of *Xanthomonadales*, *Chthoniobacterales*, and *Steroidobacterales* in the climax forest stage were significantly higher than those in the shrub, herbage, pioneer weeds, and farmland stages (Table S3).

At the family level, the relative abundances of *Xanthobacteraceae* and *Rhizobiaceae* progressively increased following old-field succession (Table S4). The relative abundances of *Solirubrobacteraceae* and *Sphingomonadaceae* were most enriched in the early forest stage. The relative abundance of *Beijerinckiaceae* in the climax forest stage was significantly lower than that in other successional stages, whereas the relative abundance of *Geodermatophilaceae* was highest and lowest in the farmland and climax forest stages, respectively. The relative abundances of *Rubrobacteriaceae* and *Roseiflexaceae* gradually declined following old-field succession, whereas the relative abundances of *Mycobacteriaceae* and *Steroidobacteraceae* in

the early and climax forest stages were significantly higher than those in other successional stages (Table S4).

At the genus level, the relative abundances of *norank_f__Xanthobacteraceae*, *Mycobacterium*, *Bradyrhizobium*, *Dongia*, and *Candidatus_Xiphinematobacter* were most enriched in the climax forest soil (Table 3). The relative abundances of *Microvirga* and *Rubrobacte* steadily decreased following old-field succession. The relative abundances of *Blastococcus* and *Arthrobacter* were highest in the farmland stage, and lowest in the climax forest stage. The relative abundances of *Gaiella* and *Bacillus* were highest in the pioneer weeds stage. The relative abundances of *Pedomicrobium* and *Phyllobacterium* in the early and climax forest stages were considerably higher than those in other successional stages (Table 3).

Table 3. Relative abundance (% of individual taxonomic groups) of the dominant bacterial genera (mean ± SE, n = 4) present in the soil (0–20 cm depth) microbial communities of different successional stages on the Loess Plateau of China.

Genus	Successional Stages						Source of Variation
	Farmland (R1)	Pioneer Weeds (R2)	Herbage (R3)	Shrub (R4)	Early Forest (R5)	Climax Forest (R6)	
Gaiella	3.17 ± 0.21 ^{b}	4.67 ± 0.21 ^{a}	3.84 ± 0.60 ^{ab}	3.68 ± 0.43 ^{ab}	3.36 ± 0.55 ^{ab}	4.24 ± 0.39 ^{ab}	n.s.
Solirubrobacter	2.32 ± 0.39 ^{a}	2.88 ± 0.51 ^{a}	2.19 ± 0.32 ^{a}	1.99 ± 0.26 ^{a}	2.73 ± 0.21 ^{a}	1.94 ± 0.31 ^{a}	n.s.
norank_f__Xanthobacteraceae	0.86 ± 0.07 ^{c}	1.14 ± 0.02 ^{c}	0.99 ± 0.07 ^{c}	1.62 ± 0.14 ^{b}	1.94 ± 0.10 ^{b}	2.53 ± 0.26 ^{a}	**
Microvirga	2.04 ± 0.16 ^{a}	1.95 ± 0.16 ^{ab}	1.71 ± 0.09 ^{ab}	1.48 ± 0.23 ^{b}	1.48 ± 0.16 ^{b}	0.48 ± 0.07 ^{c}	***
Blastococcus	3.11 ± 0.34 ^{a}	1.17 ± 0.11 ^{c}	1.35 ± 0.22 ^{bc}	1.86 ± 0.23 ^{b}	1.34 ± 0.13 ^{bc}	0.32 ± 0.02 ^{d}	**
Arthrobacter	3.08 ± 0.41 ^{a}	1.06 ± 0.05 ^{c}	1.58 ± 0.41 ^{bc}	2.41 ± 0.51 ^{ab}	1.26 ± 0.56 ^{bc}	0.60 ± 0.09 ^{c}	*
Rubrobacter	2.07 ± 0.24 ^{a}	2.36 ± 0.19 ^{a}	2.00 ± 0.33 ^{a}	1.32 ± 0.18 ^{b}	0.69 ± 0.12 ^{c}	0.26 ± 0.02 ^{c}	***
Streptomyces	1.55 ± 0.19 ^{a}	1.12 ± 0.04 ^{ab}	0.88 ± 0.10 ^{b}	1.36 ± 0.22 ^{ab}	1.18 ± 0.03 ^{ab}	1.41 ± 0.23 ^{a}	*
Mycobacterium	0.98 ± 0.10 ^{bc}	0.99 ± 0.06 ^{b}	0.77 ± 0.07 ^{c}	0.85 ± 0.09 ^{c}	1.19 ± 0.12 ^{b}	2.47 ± 0.13 ^{a}	*
Nocardioides	1.81 ± 0.56 ^{a}	0.79 ± 0.05 ^{ab}	0.62 ± 0.07 ^{b}	1.00 ± 0.21 ^{ab}	1.35 ± 0.22 ^{ab}	1.58 ± 0.43 ^{ab}	*
Bradyrhizobium	0.36 ± 0.04 ^{c}	0.52 ± 0.03 ^{c}	0.50 ± 0.08 ^{c}	0.65 ± 0.05 ^{c}	1.38 ± 0.25 ^{b}	3.20 ± 0.32 ^{a}	**
Nordella	0.62 ± 0.04 ^{c}	0.87 ± 0.05 ^{ab}	1.02 ± 0.08 ^{a}	0.75 ± 0.10 ^{bc}	0.90 ± 0.06 ^{ab}	0.61 ± 0.06 ^{c}	**
Bacillus	0.82 ± 0.16 ^{ab}	0.97 ± 0.16 ^{a}	0.75 ± 0.16 ^{ab}	0.39 ± 0.10 ^{b}	0.57 ± 0.12 ^{ab}	0.51 ± 0.06 ^{b}	n.s.
Dongia	0.49 ± 0.06 ^{b}	0.58 ± 0.07 ^{b}	0.70 ± 0.08 ^{b}	0.45 ± 0.05 ^{b}	0.71 ± 0.14 ^{b}	0.97 ± 0.05 ^{a}	**
Pseudonocardia	0.45 ± 0.05 ^{bcd}	0.40 ± 0.03 ^{cd}	0.30 ± 0.05 ^{d}	0.49 ± 0.06 ^{bc}	0.78 ± 0.06 ^{a}	0.60 ± 0.08 ^{b}	***
Pedomicrobium	0.24 ± 0.01 ^{c}	0.32 ± 0.03 ^{c}	0.30 ± 0.03 ^{c}	0.55 ± 0.04 ^{b}	0.87 ± 0.09 ^{a}	0.74 ± 0.11 ^{a}	***
Phyllobacterium	0.21 ± 0.02 ^{c}	0.38 ± 0.04 ^{b}	0.30 ± 0.02 ^{bc}	0.36 ± 0.02 ^{b}	0.77 ± 0.03 ^{a}	0.82 ± 0.09 ^{a}	**
Candidatus_Xiphinematobacter	0.09 ± 0.02 ^{b}	0.24 ± 0.04 ^{b}	0.32 ± 0.17 ^{b}	0.15 ± 0.05 ^{b}	0.41 ± 0.09 ^{b}	1.16 ± 0.28 ^{a}	*

* $p < 0.05$; ** $p < 0.01$; *** $p < 0.001$; n.s.: not significant. Different superscript lower case letters indicate statistically significant differences at the $\alpha = 0.05$ level between successional stages.

3.4. Statistically Different Bacterial Groups

LEfSe analyses were combined with LDA values to analyze the statistical significance of differentially abundant taxa for soil bacterial communities between the various successional stages (Figure 4 and Figure S2). Ten groups of bacteria enriched in the climax forest, namely, *Proteobacteria*, *Rhizobiales* (from order to family; within *Alphaproteobacteria*), *Xanthobacteraceae* (from family to genus; within *Alphaproteobacteria*), *Gammaproteobacteria*, *Bradyrhizobium* (a genus within *Rhizobiaceae*), *Mycobacteriaceae* (from family to genus; within *Actinobacteria*), *Corynebacteriales* and *Sterptosporangiales* (orders within *Actinobacteria*), *Xiphinematobacteraceae* (family to genus; within *Verrucomicrobia*), *Rokubacteria* (phylum, order, family, and genus), *Acidobacteriia* (within *Acidobacteria*), and *Mesorhizobiur* (within *Rhizobiales*) (Figure 4 and Figure S2). Soil bacterial communities in the early forest stage were enriched with *Alphaproteobacteria* (e.g., *Hyphomicrobiaceae* and *Pedomicrobium*) and *Burkholderiaceae* (within *Betaproteobacteria*). Soil bacterial taxa enriched in the shrub stage included *Gemmatimonadetes* (phylum, class, and genus), *Betaproteobacteriales* (within *Betaproteobacteria*), *Microtrichales*, *Roseiflexaceae* (from family to genus; within *Chloroflexi*), *Dehalococcoidia* (a class within *Chloroflexi*), and *Nitrosomonadaceae* (a family within *Nitrosococcales*) (Figure 4 and Figure S2). Soil bacterial taxa *Gemmatimonadales* (from order to family) and *Rubrobacterales* (from order to genus) were enriched in the herbage and pioneer weeds stages,

respectively. Soil bacterial taxa enriching the farmland stage included *Geodermatophilaceae* (e.g., *Blastococcus*; a family within *Actinobacteria*), *Frankiales* (an order within *Actinobacteria*), *Chloroflexia* (from class to order), *Thermomicrobiales* (an order within *Thermomicrobia*), *Micrococcales* (from order to family), *Arthrobacter* (a genus within *Micrococcaceae*), *Beijerinckiaceae* (a family within *Alphaproteobacteria*), *Thermomicrobiales* (an order within *Thermomicrobia*), *Propionibacteriales* (an order within *Actinobacteria*), *Nocardioidaceae* (from family to genus; within *Actinobacterales*), *Microvirga* (a genus within *Alphaproteobacteria*), *Azospirillales*, and *Streptomycetaceae* (a family within *Actinobacterales*) (Figure 4 and Figure S2).

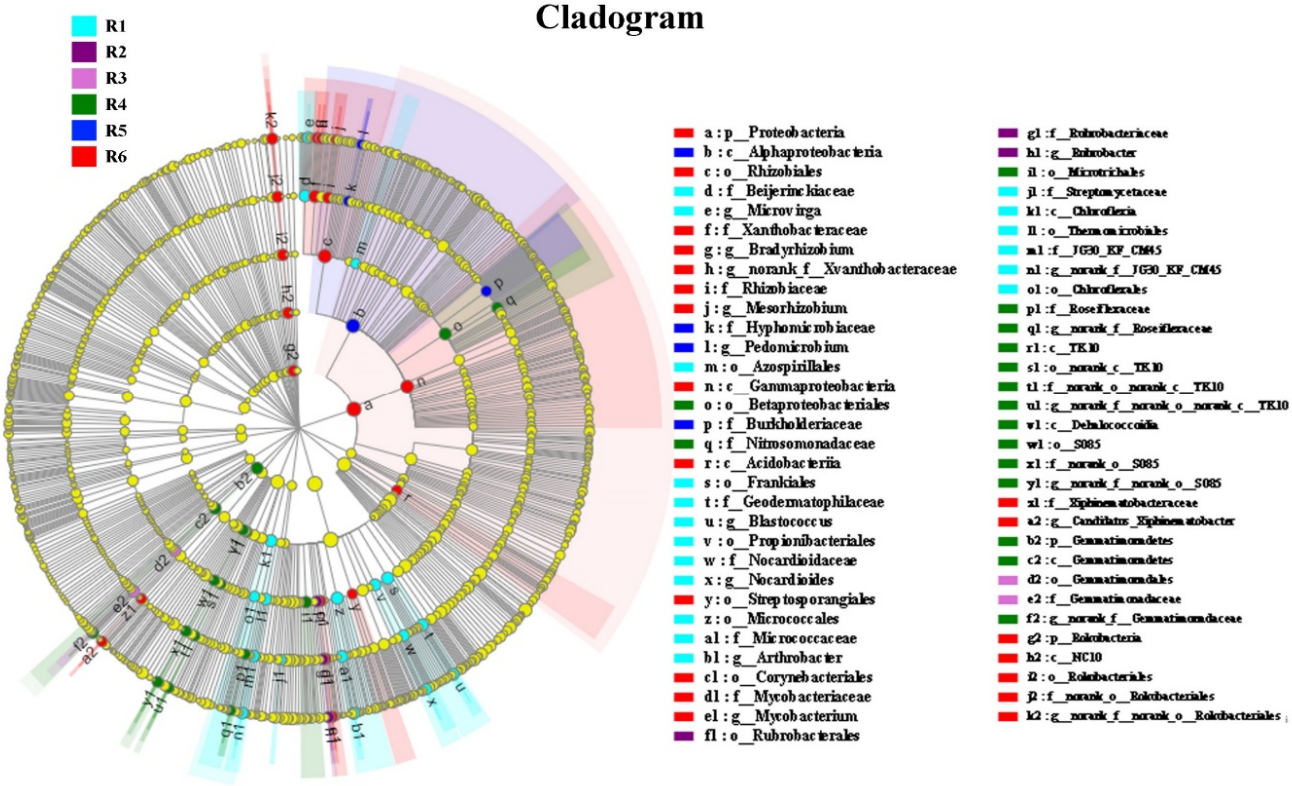

Figure 4. Cladogram indicating the phylogenetic distribution of microbial lineages associated with six different successional stages on the Loess Plateau of China; lineages with LDA values of 3.5 or higher determined by LEfSe are displayed. Differences are represented by the color of the most abundant microbial groups (In Figure 4, sky blue indicates farmland (R1), dark purple indicates pioneer weeds (R2), light purple indicates herbage (R3), green indicates shrub (R4), dark blue indicates early forest (R5), red indicates climax forest (R6), and yellow indicates non-significant). Each circle's diameter is proportional to the abundance of the taxon. Circles represent phylogenetic levels from phylum to genus, from the inside out.

3.5. Beta-Diversity of Soil Bacterial Communities

PCA analysis and Bray–Curtis similarities were employed to analyze community composition and differences in soil bacterial communities based on OTU levels, and to identify differences in bacterial communities across different successional stages (Figure 5). Both PCA analysis and Bray–Curtis similarities revealed that the climax forest soil was closely clustered together; thus, it was distinct from the early forest, shrub, herbage, pioneer weeds, and farmland stages (Figure 5a,b), indicating that climax forest soil possessed unique bacterial communities in contrast to other successional stages (Figure 5a,b). The different locations of the early forest and shrub soils tended to group together, which implied that the compositions of their bacterial communities were similar (Figure 5a,b). The herbage and pioneer weeds soils were clustered closely together, which implied that the soil bacterial community compositions of these two grasslands were similar (Figure 5a,b). Furthermore, soil bacterial community composition in the farmland stage was more similar

to pioneer weeds as well as herbage stages than the early forest and climax forest stages (Figure 5b).

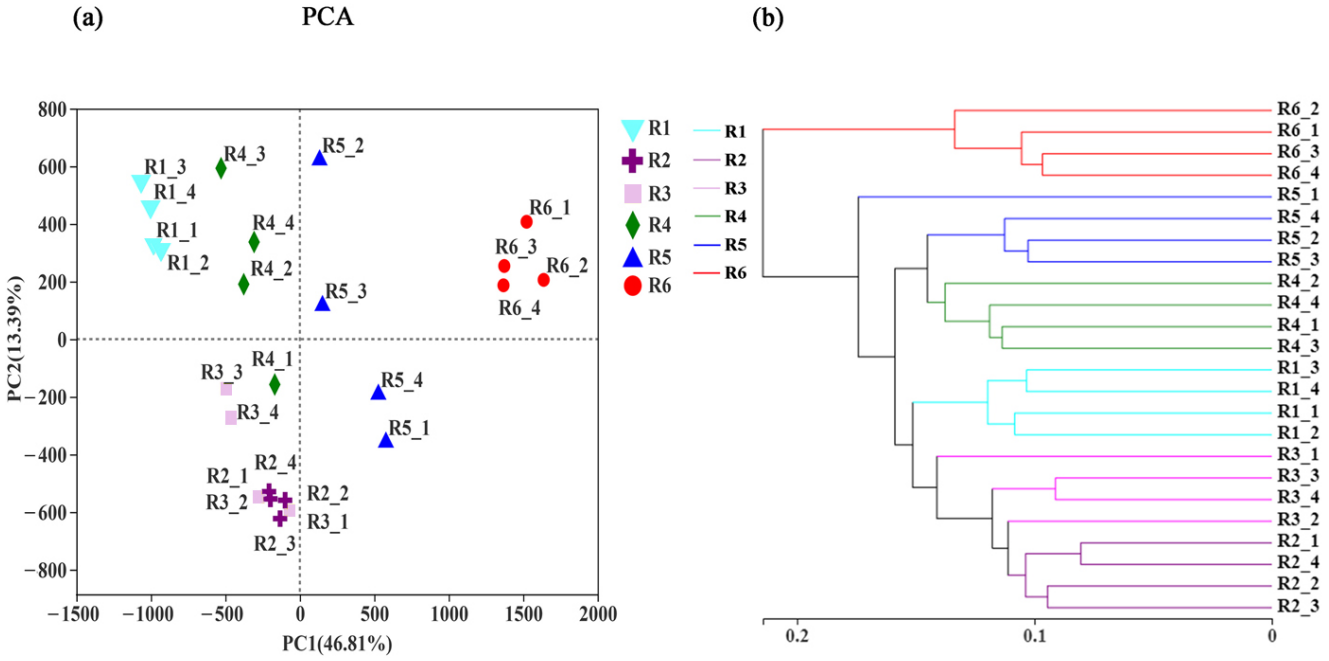

Figure 5. (**a**) Principal component analysis (PCA) and (**b**) clustering of samples. Bray–Curtis similarity index was calculated using OTU reads, and hierarchical clustering was calculated using the β-diversity distance matrix with QIIME. See Figure 2 for abbreviations.

3.6. Important Environmental Variables for Soil Bacterial Communities

Twelve environmental variables (i.e., LB, RB, soil moisture, TP, NO_3^--N, WSOC, SON, pH, NH_4^+-N, AP, TN, and SOC) explained 53.8% and 53.4% of the total changes in soil bacterial community composition at the phylum and class levels, respectively (Figure 6). The results of Monte Carlo permutation tests ($p < 0.05$) indicated that variations in soil bacterial community composition were closely related to LB ($F = 5.02$, $p = 0.0120$) and RB ($F = 3.20$, $p = 0.0490$) at the phylum level (Figure 6a) and were intimately associated with the soil WSOC ($F = 4.58$, $p = 0.0140$) at the class level (Figure 6b). Pearson's correlation analysis indicated that bacterial community abundance (i.e., 16S rRNA gene copy number) was positively correlated with LB, soil moisture, SOC, WSOC, TN, and SON, while they were negatively correlated with the pH, TP, and AP (Figure 7). The OTU richness and the species richness indices (i.e., Chao1 and ACE) of the bacterial communities were highly negatively correlated with the LB, soil moisture, SOC, WSOC, TN, and SON, and positively correlated with soil pH (Figure 7). Shannon diversity index was negatively correlated with LB, RB, SOC, and WSOC (Figure 7). The relative abundances of *Proteobacteria* and *Alphaproteobacteria* were positively correlated with LB, RB, soil moisture, SOC, WSOC, SON, and NH_4^+-N, while they were negatively correlated with the TP (Table S5; Figure 7). The relative abundances of *Chloroflexi*, *Chloroflexia*, and *Gemmatimonadetes* were significantly negatively correlated with the LB, RB, soil moisture, SOC, WSOC, SON, and NH_4^+-N, which were positively correlated with soil pH (Table S5; Figure 7). The relative abundances of *Verrucomicrobia* and *Verrucomicrobiae* were highly related to LB, moisture, SOC, TN, and SON (Table S5; Figure 7). The relative abundance of *Gammaproteobacteria* was positively correlated with the LB, soil moisture, SOC, WSOC, TN, SON, and NH_4^+-N, which was negatively correlated with the pH, TP, and AP (Table S5).

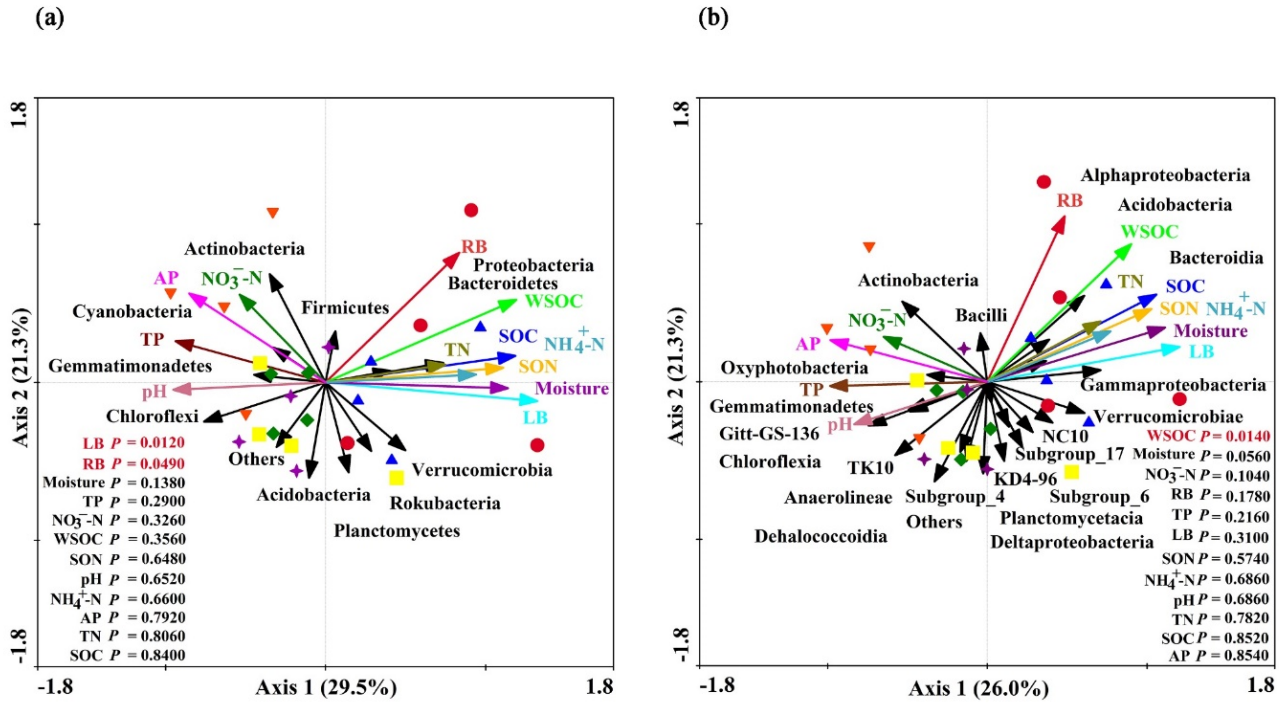

Figure 6. Redundancy analysis (RDA) diagram illustrating the relationships between the compositions of soil bacterial communities at the phylum-level (**a**) and class-level (**b**) from different sampling sites under variable environments. Explanatory variables are shown by different arrows, soil bacterial community composition by solid black arrows, and the variables of soil physiochemical properties by colored arrows: litter biomass (LB), root biomass (RB), pH, moisture, soil organic carbon (SOC), soil water-soluble organic carbon (WSOC), total nitrogen (TN), soil organic nitrogen (SON), ammonium nitrogen (NH_4^+-N), nitrate nitrogen (NO_3^--N), total phosphorus (TP), and available phosphorus (AP). Red inverted triangles represent farmland (R1) soil, dark purple stars indicate pioneer weeds (R2) soil, yellow squares represent herbage (R3) soil, green diamonds represent shrub (R4) soil, dark blue triangles represent early forest (R5) soil, and red circles represent climax forest (R6) soil.

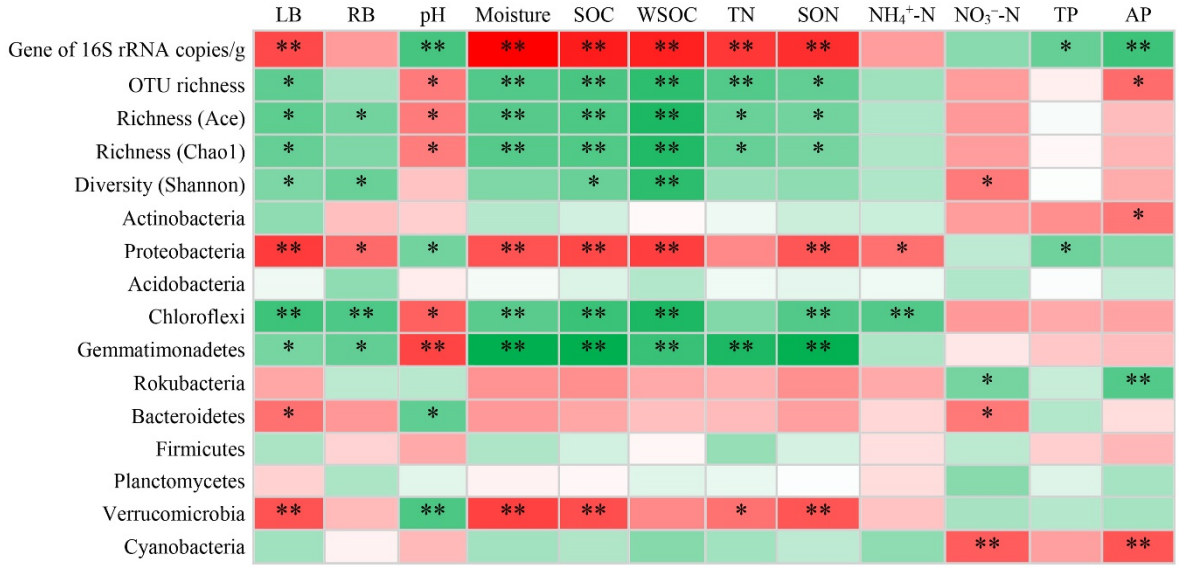

Figure 7. Pearson correlations coefficients between bacterial abundance, diversity, and community composition, and the environmental variables (n = 4) between successional stages on the Loess Plateau of China. Red indicates positive correlations, while green indicates negative correlations. The darker color, the stronger the correlation. * $p < 0.05$, ** $p < 0.01$.

4. Discussion

Our results demonstrated that secondary succession of old-field remarkably restored soil bacterial communities in degraded ecosystems, as soil bacterial abundance progressively increased following old-field succession, and reached a maximum in climax forest (Figure 2). Soil nutrient substrates (e.g., SOC, WSOC, TN, SON, and NH_4^+-N) are recognized as the overwhelming driving factors for soil bacterial abundance, owing to bacteria favoring copiotrophic environments [27,28]. In the present study, SOC, WSOC, TN, and SON concentrations gradually increased following old-field succession (Table S2). Pearson's correlation analysis indicated that soil bacterial abundance was strongly associated with litter biomass, SOC, WSOC, TN, and SON (Figure 7). Thus, the flourishing of soil bacterial abundance following old-field succession was primarily driven by the increase in soil nutrient substrates levels, which provided sufficient C, N, and energy sources for bacterial growth [56]. Additionally, soil moisture was reported to impact the growth, dormancy, and mortality of soil microbes by controlling the availability, transport, and diffusion of nutrients [39]. Generally, higher soil moisture was conducive to bacterial growth [40]. In the present study, significantly increased soil moisture was exhibited in late successional stages (Table S2), which promoted soil bacterial abundance following old-field succession (Figure 2). The secondary succession of old-field not only enhanced soil bacterial abundance, but also altered bacterial diversity on the LPC (Table 1).

It was unanticipated that the bacterial OTU richness gradually declined following old-field succession, with the lowest bacterial OTU richness, species richness, and Shannon diversity index being observed in the climax forest (Table 1). Although our findings were inconsistent with previous studies [22], they were supported by Wang et al. (2021) who revealed that soil bacterial diversity decreased during ~40 years of secondary succession in karst areas [23]. Furthermore, several studies documented that soil microbial richness increased following the conversion of native vegetation to farmland [57,58]. In the present study, soil bacterial richness and diversity were negatively correlated with litter biomass, SOC, WSOC, TN, and SON (Figure 7), which aligned with previous studies [19,23]. Soil nutrient substrates can strongly drive bacterial communities by influencing species competition and promoting the growth of functionally adapted species [59]. Soil bacterial richness and diversity declined in the late successional stages (Table 1), which was likely attributed to differences in the adaptability of distinct bacterial groups to variations in soil nutrient levels, and physiochemical properties during old-field succession (Table S2). For instance, the high level of SOM in the late successional stages possibly reduced the quantity of antagonistic bacteria in soil and decreased the soil bacterial diversity (Table S2) [23,60]. Additionally, earlier studies documented that intensity and frequency of disturbances can enhance soil microbial diversity [61,62]. Lammel et al. (2021) revealed that soil bacterial richness and diversity were considerably enhanced from pristine rainforest and Savannah to crop fields in southern Amazonia, owing to the continual disturbances that occurred in crop fields [62]. We deduced that the highest soil bacterial OTU richness was in the farmland stage (Table 1), which likely resulted from frequent anthropogenic disturbances that stimulated the bacterial OTU richness [61,62].

Secondary succession of old-field was observed to significantly modify the composition of soil bacterial communities (Figure 5a,b). The PCA index and Bray–Curtis similarity index showed that soil bacterial community composition was gradually altered from the early, medium term, and late successional stages, to ultimately where climax forest was significantly distinct from other successional stages (Figure 5a,b). RDA analyses displayed that variations in soil bacterial community composition at the phylum and class levels were strongly correlated with LB, RB, and WSOC (Figure 6a,b). This further confirmed that litter, root biomass, and WSOC were overarching driving factors for variation in soil bacterial community composition [40,59]. Plant-specific traits (e.g., litter and root) contributed significantly to soil nutrient availability by supplying plentiful C-rich compounds to the soil [63,64]. WSOC is a key fraction of the soil labile organic C pool, which is considered to be a direct reservoir of easily assimilable C for microbial growth and metabolism [49].

Francioli et al. (2016) showed that different bacterial community taxa exhibited distinct responses to the availability of nutrients in soils [34]. It was presumed that changes in soil nutrient availability and plant traits following old-field succession likely triggered variations in soil bacterial community composition (Table 2) [34].

Actinobacteria and *Proteobacteria* were the most predominant phyla across all successional stages (Figure 3). This aligned with previous studies, which showed that these two ubiquitous bacterial taxa generally dominated the majority of soils [2,65]. Following old-field succession, the relative abundance of *Proteobacteria* steadily increased, while that of *Actinobacteria* decreased slightly (Figure 3). Although most *Actinobacteria* are saprophytes [66], they prefer and thrive in oligotrophic environments by providing a series of extracellular hydrolytic enzymes [67,68]. These enzymes have the capacity to degrade plant and animal residues [62], as well as highly recalcitrant organic materials [69], which enables *Actinobacteria* to flourish in resource-limited conditions [68]. LEfSe analyses and LDA values indicted that the most abundant members of *Actinobacteria*, including *Geodermatophilaceae*, *Frankiales*, *Blastococcus*, *Micrococcales*, *Micrococcacea*, *Propionibacteriales*, *Nocardioidaceae*, *Nocardioide*, and *Streptomycetacea*, were present in the farmland stage (Figure 4 and Figure S2), which likely resulted from the lower levels of available nutrient substrates in the farmland stage relative to other successional stages (Table S2). Furthermore, most *Actinomycetes* prefer aerobic environments [70]. Thus, abundant litter biomass and soil moisture following old-field succession may lead to poor soil aeration and lower oxygen content (Table S2), which inhibits *Actinomycete* proliferation (Figure 3).

It was shown that the progressively increased relative abundance of *Proteobacteria* following old-field succession was primarily due to the enrichment of *Alphaproteobacteria* and *Gammaproteobacteria*, rather than *Deltaproteobacteria* (Table 2). *Proteobacteria* (e.g., *Alphaproteobacteria* and *Gammaproteobacteria*) are known to be fast-growing copiotrophic groups, abundant in soil with sufficient labile substrates [37,45,71,72]. This was supported by our findings that *Proteobacteria*, *Alphaproteobacteria*, and *Gammaproteobacteria* were strongly associated with LB, SOC, WSOC, SON, and NH_4^+-N (Table S5; Figure 7). LEfSe analyses and LDA values indicated that the most abundant members of *Proteobacteria* (e.g., *Rhizobiales*, *Xanthobacteraceae*, *Gammaproteobacteria*, *Bradyrhizobium*, *Rhizobiaceae*, and *Mesorhizobiur*) were observed in climax forest (Figure 4 and Figure S2). We extrapolated that gradually increased members of *Proteobacteria* following old-field succession were largely driven by the considerably enhanced availability of resources [37].

In this study, the *Rhizobiales* order was the largest subgroup within *Alphaproteobacteria* across all successional stages (Table S3 and Table 2). The proportion of *Rhizobiales* in the *Alphaproteobacteria* gradually increased following old-field succession, which accounted for 53.29%, 58.32%, 55.70%, 64.31%, 64.06%, and 69.92% in the farmland, pioneer weeds, herbage, shrub, early forest, and climax forest stages, respectively (Table S3 and Table 2). LEfSe analyses and LDA values confirmed that significant enrichment of *Rhizobiales*, *Rhizobiaceae*, and *Bradyrhizobium* was observed in the climax forest (Figure 4 and Figure S2). Previous studies reported that the members of *Rhizobiales* (from order to genus) were greatly affected by soil pH [73]. *Rhizobiales* was affiliated within *Alphaproteobacteria*, showing an opposite trend with increasing soil pH [74]. Moreover, *Rhizobiales* was shown to be positively correlated with SOC fractions [75]. It was deduced that the most enriched members of *Rhizobiales* found in climax forest may have been intimately associated with the lowest soil pH, and the highest SOC and WSOC (Figure 4 and Figure S2). The members of *Rhizobiales* contain many N-fixing endophytes [63,76], have the ability to supply N for its symbiotic plant by fixing atmospheric N [77], and play key roles in the promotion of plant growth [76]. Further, *Rhizobiales* members are extensively involved in N fixation [77] and the decomposition of OM [26]. It may be surmised that greatly increased members of *Rhizobiales* in the late successional stages provide ample N nutrition to symbiotic plants through the fixation of atmospheric N to promote their primary productivity (Table 3, Tables S3 and S4) [76,77]. Ultimately, they indirectly facilitate the accumulation of SOC and SON owing to additional plant residues returning to the soil (Table S2). Similarly, the *Xanthomonadales* order within

Gammaproteobacteria has been documented to favor soil environments with low pH [26]. The highest relative abundance of *Xanthomonadales* in climax forest may be partially attributed to the lower soil pH between successional stages (Tables S2 and S3). Furthermore, with the relative abundance of *Acidobacteria*, little changed following old-field succession, revealing that alterations of soil nutrient substrates and physicochemical properties had no significant impact on *Acidobacteria* in this study (Figure 3).

In general, *Chloroflexi*, *Gemmatimonadetes*, *Firmicutes*, and *Cyanobacteria* are widely regarded as slow-growing oligotrophic groups that flourish in nutrient-deprived and disturbed environments [4,35,36,78]. *Chloroflexi* belong to photoautotrophic bacteria [40] and can fix C through photosynthesis [79]. Trivedi et al. (2016) documented that *Chloroflexi* was more enriched in agricultural systems relative to natural systems [80]. In this study, the lower *Chloroflexi* abundance (from phylum to class) in climax forest was primarily caused by the highest soil nutrient substrates levels, which restricted the oligotrophic *Chloroflexi* (Table 2 and Table S2; Figure 3). Moreover, the increased canopy density in climax forest reduced the light intensity that might be negatively affected photosynthesis for *Chloroflexi* and the growth of *Chloroflexi* (Table S1) [9]. Members of *Firmicutes*, particularly *Bacilli* (from class to genus), have been documented to survive in harsh environments that were instrumental in Endospore-forming *Firmicutes*, which carried out various survival strategies to resist disadvantaged circumstances [81]. It was deduced that the low level of SOM and harsh environments in the farmland and pioneer weeds stages might have stimulated the growth of *Firmicutes*, which resulted in higher relative abundances of *Firmicutes* and *Bacilli* (from class to genus) compared with other successional stages (Table 2, Table 3 and Tables S2–S4; Figure 3). Additionally, *Cyanobacteria* and *Oxyphotobacteria* (a class within *Cyanobacteria*) are well-known photoautotrophs with desiccation-resistant features [82], which have been shown to flourish under greater solar radiation and lower soil moisture [82]. In the present study, *Cyanobacteria* and *Oxyphotobacteria* were most abundant in the farmland stage, while they significantly declined following old-field succession (Table 2; Figure 3). It was reasoned that substantially decreased *Cyanobacteria* and *Oxyphotobacteria* abundance following old-field succession may have partly resulted from a gradually decrease in the availability of sunlight owing to greater shading caused by the canopies of shrubs and trees and increased litter coverage (Table 2 and Table S2; Figure 3) [83]. *Cyanobacteria* and some members of *Firmicutes* (e.g., members of *Bacillales*) have been documented to be N fixing species; thus, it may be surmised that the most enriched *Cyanobacteria* and *Firmicutes* abundance would facilitate supply and absorption of soil nutrients in the farmland stage (Table S2; Figure 3) [84,85].

Shifts in soil bacterial community composition can affect decomposition and sequestration of SOM [40]. In the present study, LEfSe and ANOVA analyses displayed that the soil bacterial community composition was transformed from oligotrophic groups (e.g., *Actinobacteria*, *Firmicutes*, and *Cyanobacteria*) to copiotrophic groups (e.g., *Proteobacteria*) following old-field succession (Figure 3, Figure 4 and Figure S2). Oligotrophic bacteria have been shown to favor the decay of recalcitrant organic materials [36,69,86]. For instance, Barka et al. (2016) reported that *Actinobacteria* have the capacity to degrade highly recalcitrant organic compounds through the penetration of their hypha into plant tissues [69]. *Chloroflexi* plays a central role in degradation of recalcitrant matter (e.g., aromatics, N-containing, and phenolic compounds) [86]. Lladó et al. (2017) revealed that *Firmicutes* have the ability to utilize recalcitrant C [36]. The highest abundance of oligotrophic bacteria (e.g., *Actinobacteria* and *Firmicutes*) in the farmland stage likely accelerated the decomposition of recalcitrant OM which had a prolonged residence time [36,69]. This facilitates the decomposition of SOM, which may be detrimental SOC and SON sequestration in the long-term [87,88]. Conversely, copiotrophic bacteria, particularly *Proteobacteria*, thrive in nutrient-rich environments with a high availability of C [37,71], and have a preference for the decomposition of labile OM owing to only sufficient labile C substrates ensuring their rapid growth rate [72]. It may be postulated that the climax forest possessed the most abundant copiotrophic *Proteobacteria*, and less oligotrophic *Chloroflexi*, *Gemmatimonadetes*,

and *Actinobacteria* relative to farmland stage (Figure 3). This might promote the SOC and SON accumulation by increasing utilization of labile organic C and N, while decelerating the decomposition of recalcitrant organic C and N following old-field succession (Table S2) [69,72,86].

5. Conclusions

The study revealed that soil bacterial abundance progressively increased, while bacterial richness and diversity significantly decreased following ~160 years of old-field succession. The composition of soil bacterial communities was transformed from oligotrophic groups to copiotrophic groups following old-field succession. This transformation was primarily driven by variations in litter and root biomass, soil nutrient substrates, physicochemical properties, and light intensity. Climax forest exhibited the most abundant copiotrophic *Proteobacteria*, and less oligotrophic *Actinobacteria*, *Chloroflexi*, and *Gemmatimonadetes* relative to farmland stage. This likely promoted SOC and SON sequestration over the long-term through raising utilization of labile organic C and N and decreasing recalcitrant organic C and N decomposition along with old-field succession. This study provides evidence toward better elucidating variations and driving mechanisms behind changes in soil bacterial communities following old-field succession, which will provide policymakers with a scientific basis for evaluating the effectiveness of ecological restoration strategy from the perspective of soil microbial recovery to promote restoration and sustainable management of degraded ecosystems.

Supplementary Materials: The following supporting information can be downloaded at: https://www.mdpi.com/article/10.3390/f13101628/s1, Table S1: Geographical features and vegetation at different successional stages on the Loess Plateau of China, Table S2: Plant and soil (0–20 cm depth) properties (mean ± SE, n = 4) at different successional stages on the Loess Plateau of China, Table S3: Relative abundance (% of individual taxonomic groups) of the dominant bacterial orders (mean ± SE, n = 4) present in the soil (0–20 cm depth) microbial communities at different successional stages on the Loess Plateau of China, Table S4: Relative abundance (% of individual taxonomic groups) of the dominant bacterial families (mean ± SE, n = 4) present in the soil (0–20 cm depth) microbial communities at different successional stages on the Loess Plateau of China, Table S5: Pearson correlations coefficients between soil bacterial communities at the class-level and the environmental variables (n = 4) between successional stages on the Loess Plateau of China, Figure S1: α-Diversity comparison. (a) Rarefaction curves for OTU and (b) Shannon-Wiener curves were calculated using Mothur (v.1.30.1) with reads normalized to 40,838 for each sample using 0.03 distance OTU. See Figure 2 for abbreviations, Figure S2: Indicator microbial groups within six different successional stages with LDA values higher than 3.5. See Figure 2 for abbreviations.

Author Contributions: W.Y. performed the experiment, analysed the data, and drafted the manuscript. X.C. (Xinwen Cai), Y.W. and L.D. participated in the main experiments. L.X., S.A. and Y.L. reviewed the manuscript and contributed to revisions. W.Y. and X.C. (Xiaoli Cheng) designed the study and revised the manuscript. All authors have read and agreed to the published version of the manuscript.

Funding: This work was supported by the National Natural Science Foundation of China (grant no. 32071632; 31600427), the Natural Science Foundation of Shaanxi Province, China (grant no. 2022JM-114; 2019JQ-666), and the Fundamental Research Funds for the Central Universities (grant no. GK202003051).

Institutional Review Board Statement: Not applicable.

Informed Consent Statement: Not applicable.

Data Availability Statement: Data may be obtained upon request from the authors.

Conflicts of Interest: The authors declare no conflict of interest.

References

1. Khorchani, M.; Nadal-Romero, E.; Lasanta, T.; Tague, C. Carbon sequestration and water yield tradeoffs following restoration of abandoned agricultural lands in Mediterranean mountains. *Environ. Res.* **2022**, *207*, 112203. [CrossRef] [PubMed]
2. Zhang, Z.; Han, X.; Yan, J.; Zou, W.; Wang, E.; Lu, X.; Chen, X. Keystone microbiomes revealed by 14 years of field restoration of the degraded agricultural soil under distinct vegetation scenarios. *Front. Microbiol.* **2020**, *11*, 1915. [CrossRef]
3. Campbell, J.E.; Lobell, D.B.; Genova, R.C.; Field, C.B. The global potential of bioenergy on abandoned agriculture lands. *Environ. Sci. Technol.* **2008**, *42*, 5791–5794. [CrossRef] [PubMed]
4. Csecserits, A.; Czucz, B.; Halassy, M.; Kroel-Dulay, G.; Redei, T.; Szabo, R.; Szitar, K.; Torok, K. Regeneration of sandy old-fields in the forest steppe region of Hungary. *Plant Biosyst.* **2011**, *145*, 715–729. [CrossRef]
5. Yan, B.; Sun, L.; Li, J.; Liang, C.; Wei, F.; Xue, S.; Wang, G. Change in composition and potential functional genes of soil bacterial and fungal communities with secondary succession in *Quercus liaotungensis* forests of the Loess Plateau, western China. *Geoderma* **2020**, *364*, 114199. [CrossRef]
6. Sullivan, B.; Nifong, R.; Nasto, M.K.; Alvarez-Clare, S.; Dencker, C.M.; Soper, F.M.; Shoemaker, K.T.; Ishida, F.Y.; Zaragoza-Castells, J.; Davidson, E.A.; et al. Biogeochemical recuperation of lowland tropical forest during succession. *Ecology* **2019**, *10*, e02641. [CrossRef] [PubMed]
7. Zhang, C.; Liu, G.; Song, Z.; Qu, D.; Fang, L.; Deng, L. Natural succession on abandoned cropland effectively decreases the soil erodibility and improves the fungal diversity. *Ecol. Appl.* **2017**, *27*, 2142–2154. [CrossRef] [PubMed]
8. Bullock, J.M.; Aronson, J.; Newton, A.C.; Pywell, R.F.; Rey-Benayas, J.M. Restoration of ecosystem services and biodiversity: Conflicts and opportunities. *Trends Ecol. Evol.* **2011**, *26*, 541–549. [CrossRef] [PubMed]
9. Lozano, Y.M.; Hortal, S.; Armas, C.; Pugnaire, F.I. Interactions among soil, plants, and microorganisms drive secondary succession in a dry environment. *Soil Biol. Biochem.* **2014**, *78*, 298–306. [CrossRef]
10. Krishna, M.; Gupta, S.; Delgado–Baquerizo, M.; Morriën, E.; Garkoti, S.C.; Chaturvedi, R.; Ahmad, S. Successional trajectory of bacterial communities in soil are shaped by plant-driven changes during secondary succession. *Sci. Rep.* **2020**, *10*, 9864. [CrossRef]
11. Kuramae, E.E.; Gamper, H.A.; Yergeau, E.; Piceno, Y.M.; Brodie, E.L.; DeSantis, T.Z.; Andersen, G.L.; van Veen, J.A.; Kowalchuk, G.A. Microbial secondary succession in a chronosequence of chalk grasslands. *ISME J.* **2010**, *4*, 711–715. [CrossRef] [PubMed]
12. Kardol, P.; Bezemer, T.M.; van der Putten, W.H. Temporal variation in plant-soil feedback controls succession. *Ecol. Lett.* **2006**, *9*, 1080–1088. [CrossRef] [PubMed]
13. Wagg, C.; Schlaeppi, K.; Banerjee, S.; Kuramae, E.E.; van der Heijden, M.G. Fungal-bacterial diversity and microbiome complexity predict ecosystem functioning. *Nat. Commun.* **2019**, *10*, 4841. [CrossRef]
14. Rousk, J.; Bååth, E.; Brookes, P.C.; Lauber, C.L.; Lozupone, C.; Caporaso, J.G.; Knight, R.; Fierer, N. Soil bacterial and fungal communities across a pH gradient in an arable soil. *ISME J.* **2010**, *4*, 1340–1351. [CrossRef] [PubMed]
15. Jurburg, S.D.; Natal-da-Luz, T.; Raimundo, J.; Morais, P.V.; Sousa, J.P.; van Elsas, J.D.; Salles, J.F. Bacterial communities in soil become sensitive to drought under intensive grazing. *Sci. Total Environ.* **2018**, *618*, 1638–1646. [CrossRef] [PubMed]
16. DeCrappeo, N.M.; DeLorenze, E.J.; Giguere, A.T.; Pyke, D.A.; Bottomley, P.J. Fungal and bacterial contributions to nitrogen cycling in cheatgrass-invaded and uninvaded native sagebrush soils of the western USA. *Plant Soil* **2017**, *416*, 271–281. [CrossRef]
17. Schimel, J.; Becerra, C.A.; Blankinship, J. Estimating decay dynamics for enzyme activities in soils from different ecosystems. *Soil Biol. Biochem.* **2017**, *114*, 5–11. [CrossRef]
18. Zeng, Q.; Liu, Y.; Zhang, H.; An, S. Fast bacterial succession associated with the decomposition of Quercus wutaishanica litter on the Loess Plateau. *Biogeochemistry* **2019**, *144*, 119–131. [CrossRef]
19. Schlatter, D.C.; Bakker, M.G.; Bradeen, J.M.; Kinkel, L.L. Plant community richness and microbial interactions structure bacterial communities in soil. *Ecology* **2015**, *96*, 134–142. [CrossRef]
20. Waymouth, V.; Miller, R.E.; Kasel, S.; Ede, F.; Bissett, A.; Aponte, C. Soil bacterial community responds to land-use change in riparian ecosystems. *Forests* **2021**, *12*, 157. [CrossRef]
21. Zhang, C.; Liu, G.; Xue, S.; Wang, G. Soil bacterial community dynamics reflect changes in plant community and soil properties during the secondary succession of abandoned farmland in the Loess Plateau. *Soil Biol. Biochem.* **2016**, *97*, 40–49. [CrossRef]
22. Zhong, Z.; Zhang, X.; Wang, X.; Fu, S.; Wu, S.; Lu, X.; Ren, C.; Han, X.; Yang, G. Soil bacteria and fungi respond differently to plant diversity and plant family composition during the secondary succession of abandoned farmland on the Loess Plateau, China. *Plant Soil* **2020**, *448*, 183–200. [CrossRef]
23. Wang, G.; Liu, Y.; Cui, M.; Zhou, Z.; Zhang, Q.; Li, Y.; Ha, W.; Pang, D.; Luo, J.; Zhou, J. Effects of secondary succession on soil fungal and bacterial compositions and diversities in a karst area. *Plant Soil* **2022**, *475*, 91–102. [CrossRef]
24. Hu, P.; Xiao, J.; Zhang, W.; Xiao, L.; Yang, R.; Xiao, D.; Zhao, J.; Wang, K. Response of soil microbial communities to natural and managed vegetation restoration in a subtropical karst region. *Catena* **2020**, *195*, 104849. [CrossRef]
25. Lange, M.; Eisenhauer, N.; Sierra, C.A.; Bessler, H.; Engels, C.; Griffiths, R.; Mellado-Vázquez, P.G.; Malik, A.A.; Roy, J.; Scheu, S.; et al. Plant diversity increases soil microbial activity and soil carbon storage. *Nat. Commun.* **2015**, *6*, 6707. [CrossRef]
26. Dukunde, A.; Schneider, D.; Schmidt, M.; Veldkamp, E.; Daniel, R. Tree species shape soil bacterial community structure and function in temperate deciduous forests. *Front. Microbiol.* **2019**, *10*, 1519. [CrossRef] [PubMed]
27. Santonja, M.; Fernandez, C.; Proffit, M.; Gers, C.; Gauquelin, T.; Reiter, I.M.; Cramer, W.; Baldy, V. Plant litter mixture partly mitigates the negative effects of extended drought on soil biota and litter decomposition in a Mediterranean oak forest. *J. Ecol.* **2017**, *105*, 801–815. [CrossRef]

28. Peguero, G.; Folch, E.; Liu, L.; Ogaya, R.; Peñuelas, J. Divergent effects of drought and nitrogen deposition on microbial and arthropod soil communities in a Mediterranean forest. *Eur. J. Soil Biol.* **2021**, *103*, 103275. [CrossRef]
29. Nguyen, L.T.T.; Osanai, Y.; Lai, K.; Anderson, I.C.; Bange, M.P.; Tissue, D.T.; Singh, B.K. Responses of the soil microbial community to nitrogen fertilizer regimes and historical exposure to extreme weather events: Flooding or prolonged-drought. *Soil Biol. Biochem.* **2018**, *118*, 227–236. [CrossRef]
30. Keet, J.H.; Ellis, A.G.; Hui, C.; Le Roux, J.J. Strong spatial and temporal turnover of soil bacterial communities in South Africa's hyperdiverse fynbos biome. *Soil Biol. Biochem.* **2019**, *136*, 107541. [CrossRef]
31. Bainard, L.D.; Hamel, C.; Gan, Y.T. Edaphic properties override the influence of crops on the composition of the soil bacterial community in a semiarid agroecosystem. *Appl. Soil Ecol.* **2016**, *105*, 160–168. [CrossRef]
32. Cheng, J.; Zhao, M.; Cong, J.; Qi, Q.; Xiao, Y.; Cong, W.; Deng, Y.; Zhou, J.; Zhang, Y. Soil pH exerts stronger impacts than vegetation type and plant diversity on soil bacterial community composition in subtropical broad-leaved forests. *Plant Soil.* **2020**, *450*, 273–286. [CrossRef]
33. Zhalnina, K.; Louie, K.B.; Hao, Z.; Mansoori, N.; da Rocha, U.N.; Shi, S.; Cho, H.; Karaoz, U.; Loqué, D.; Bowen, B.P.; et al. Dynamic root exudate chemistry and microbial substrate preferences drive patterns in rhizosphere microbial community assembly. *Nat. Microbiol.* **2018**, *3*, 470–480. [CrossRef]
34. Francioli, D.; Schulz, E.; Lentendu, G.; Wubet, T.; Buscot, F.; Reitz, T. Mineral vs. organic amendments: Microbial community structure, activity and abundance of agriculturally relevant microbes are driven by long-term fertilization strategies. *Front. Microbiol.* **2016**, *7*, 1446. [CrossRef] [PubMed]
35. Koyama, A.; Wallenstein, M.D.; Simpson, R.T.; Moore, J.C. Soil bacterial community composition altered by increased nutrient availability in Arctic tundra soils. *Front. Microbiol.* **2014**, *5*, 516. [CrossRef]
36. Lladó, S.; López-Mondéjar, R.; Baldrian, P. Forest soil bacteria: Diversity, involvement in ecosystem processes, and response to global change. *Microbiol Mol. Biol. Rev.* **2017**, *81*, e00063-16. [CrossRef] [PubMed]
37. Fierer, N.; Lauber, C.L.; Ramirez, K.S.; Zaneveld, J.; Bradford, M.A.; Knight, R. Comparative metagenomic, phylogenetic and physiological analyses of soil microbial communities across nitrogen gradients. *ISME J.* **2012**, *6*, 1007–1017. [CrossRef]
38. Verzeaux, J.; Alahmad, A.; Habbib, H.; Nivelle, E.; Roger, D.; Lacoux, J.; Decocq, G.; Hirel, B.; Catterou, M.; Spicher, F.; et al. Cover crops prevent the deleterious effect of nitrogen fertilisation on bacterial diversity by maintaining the carbon content of ploughed soil. *Geoderma* **2016**, *281*, 49–57. [CrossRef]
39. Ullah, M.R.; Carrillo, Y.; Dijkstra, F.A. Drought-induced and seasonal variation in carbon use efficiency is associated with fungi:bacteria ratio and enzyme production in a grassland ecosystem. *Soil Biol. Biochem.* **2021**, *155*, 108159. [CrossRef]
40. Yang, W.; Cai, A.; Wang, J.; Luo, Y.; Cheng, X.; An, S. Exotic *Spartina alterniflora* Loisel. Invasion significantly shifts soil bacterial communities with the successional gradient of saltmarsh in eastern China. *Plant Soil* **2020**, *449*, 97–115. [CrossRef]
41. Fu, B.; Liu, Y.; Lu, Y.; He, C.; Zeng, Y.; Wu, B. Assessing the soil erosion control service of ecosystems change in the Loess Plateau of China. *Ecol. Complex.* **2011**, *8*, 284–293. [CrossRef]
42. Deng, L.; Liu, G.B.; Shangguan, Z.P. Land-use conversion and changing soil carbon stocks in China's 'Grain-for-Green' Program: A synthesis. *Glob. Chang. Biol.* **2014**, *20*, 3544–3556. [CrossRef] [PubMed]
43. Deng, L.; Kim, D.; Peng, C.H.; Shuangguan, Z.P. Controls of soil and aggregate-associated organic carbon variations following natural vegetation restoration on the Loess Plateau in China. *Land Degrad. Dev.* **2018**, *29*, 3974–3984. [CrossRef]
44. Gao, G.; Tuo, D.; Han, X.; Jiao, L.; Li, J.; Fu, B. Effects of land-use patterns on soil carbon and nitrogen variations along revegetated hillslopes in the Chinese Loess Plateau. *Sci. Total Environ.* **2020**, *746*, 141156. [CrossRef] [PubMed]
45. Han, X.; Ren, C.; Li, B.; Yan, S.; Fu, S.; Gao, D.; Zhao, F.; Deng, J.; Yang, G. Growing seasonal characteristics of soil and plants control the temporal patterns of bacterial communities following afforestation. *Catena* **2019**, *178*, 288–297. [CrossRef]
46. Zhong, Y.; Yan, W.; Wang, R.; Wang, W.; Shangguan, Z. Decreased occurrence of carbon cycle functions in microbial communities along with long-term secondary succession. *Soil Biol. Biochem.* **2018**, *123*, 207–217. [CrossRef]
47. Chen, C. The vegetation and its roles in soil and water conservation in the secondary forest area in the boundary of Shaanxi and Gansu provinces. *Acta Phytoecol. Geobot. Sin.* **1954**, *2*, 152–153.
48. Wang, J.; Zhao, W.; Zhang, X.; Liu, Y.; Wang, S.; Liu, Y. Effects of reforestation on plant species diversity on the Loess Plateau of China: A case study in Danangou catchment. *Sci. Total Environ.* **2019**, *651*, 979–989. [CrossRef]
49. Yang, W.; Yan, Y.; Jiang, F.; Leng, X.; Cheng, X.; An, S. Response of the soil microbial community composition and biomass to a short-term *Spartina alterniflora* invasion in a coastal wetland of eastern China. *Plant Soil* **2016**, *408*, 443–456. [CrossRef]
50. Sun, R.; Zhang, X.; Guo, X.; Wang, D.; Chu, H. Bacterial diversity in soils subjected to long-term chemical fertilization can be more stably maintained with the addition of livestock manure than wheat straw. *Soil Biol. Biochem.* **2015**, *88*, 9–18. [CrossRef]
51. Caporaso, J.G.; Kuczynski, J.; Stombaugh, J.; Bittinger, K.; Bushman, F.D.; Costello, E.K.; Fierer, N.; Peña, A.G.; Goodrich, J.K.; Gordon, J.I.; et al. QIIME allows analysis of high-throughput community sequencing data. *Nat. Methods* **2010**, *7*, 335–336. [CrossRef] [PubMed]
52. Bolger, A.M.; Lohse, M.; Usadel, B. Trimmomatic: A flexible trimmer for Illumina sequence data. *Bioinformatics* **2014**, *30*, 2114–2120. [CrossRef] [PubMed]
53. Edgar, R.C. UPARSE: Highly accurate OTU sequences from microbial amplicon reads. *Nat. Methods* **2013**, *10*, 996–998. [CrossRef] [PubMed]

54. Schloss, P.D.; Westcott, S.L.; Ryabin, T.; Hall, J.R.; Hartmann, M.; Hollister, E.B.; Lesniewski, R.A.; Oakley, B.B.; Parks, D.H.; Robinson, C.J.; et al. Introducing mothur: Open-source, platform-independent, community-supported software for describing and comparing microbial communities. *Appl. Environ. Microbiol.* **2009**, *75*, 7537–7541. [CrossRef] [PubMed]
55. Cole, J.R.; Wang, Q.; Cardenas, E.; Fish, J.; Chai, B.; Farris, R.J.; Kulam-Syed-Mohideen, A.S.; McGarrell, D.M.; Marsh, T.; Garrity, G.M.; et al. The Ribosomal Database Project: Improved alignments and new tools for rRNA analysis. *Nucleic Acids Res.* **2009**, *37*, 141–145. [CrossRef] [PubMed]
56. Rodriguez-Caballero, G.; Caravaca, F.; Alguacil, M.M.; Fernandez-Lopez, M.; Fernandez-Gonzalez, A.J.; Roldan, A. Striking alterations in the soil bacterial community structure and functioning of the biological N cycle induced by Pennisetum setaceum invasion in a semiarid environment. *Soil Biol. Biochem.* **2017**, *109*, 176–187. [CrossRef]
57. George, P.B.L.; Lallias, D.; Creer, S.; Seaton, F.M.; Kenny, J.G.; Eccles, R.M.; Griffiths, R.I.; Lebron, I.; Emmett, B.A.; Robinson, D.A.; et al. Divergent national-scale trends of microbial and animal biodiversity revealed across diverse temperate soil ecosystems. *Nat. Commun.* **2019**, *10*, 1107. [CrossRef] [PubMed]
58. Pedrinho, A.; Mendes, L.W.; Merloti, L.F.; da Fonseca, M.D.C.; Cannavan, F.D.S.; Tsai, S.M. Forest-to-pasture conversion and recovery based on assessment of microbial communities in Eastern Amazon rainforest. *FEMS Microbiol. Ecol.* **2019**, *95*, fiy236. [CrossRef]
59. Cassman, N.A.; Leite, M.F.A.; Pan, Y.; de Hollander, M.; van Veen, J.A.; Kuramae, E.E. Plant and soil fungal but not soil bacterial communities are linked in long-term fertilized grassland. *Sci. Rep.* **2016**, *6*, 23680. [CrossRef] [PubMed]
60. Bakker, M.G.; Otto-Hanson, L.; Lange, A.J.; Bradeen, J.M.; Kinkel, L.L. Plant monocultures produce more antagonistic soil Streptomyces communities than high-diversity plant communities. *Soil Biol. Biochem.* **2013**, *65*, 304–312. [CrossRef]
61. Santillan, E.; Seshan, H.; Constancias, F.; Drautz-Moses, D.I.; Wuertz, S. Frequency of disturbance alters diversity, function, and underlying assembly mechanisms of complex bacterial communities. *npj Biofilms Microbiomes* **2019**, *5*, 8. [CrossRef] [PubMed]
62. Lammel, D.R.; Nüsslein, K.; Cerri, C.E.P.; Veresoglou, S.D.; Rillig, M.C. Soil biota shift with land use change from pristine rainforest and Savannah (Cerrado) to agriculture in southern Amazonia. *Mol. Ecol.* **2021**, *30*, 4899–4912. [CrossRef] [PubMed]
63. Byers, A.K.; Condron, L.; Donavan, T.; O'Callaghan, M.; Patuawa, T.; Waipara, N.; Black, A. Soil microbial diversity in adjacent forest systems-contrasting native, old growth kauri (*Agathis australis*) forest with exotic pine (*Pinus radiata*) plantation forest. *FEMS Microbiol. Ecol.* **2020**, *96*, fiaa047. [CrossRef] [PubMed]
64. Picariello, E.; Baldantoni, D.; Izzo, F.; Langella, A.; De Nicola, F. Soil organic matter stability and microbial community in relation to different plant cover: A focus on forests characterizing Mediterranean area. *Appl. Soil Ecol.* **2021**, *162*, 103897. [CrossRef]
65. Bell, C.W.; Asao, S.; Calderon, F.; Wolk, B.; Wallenstein, M.D. Plant nitrogen uptake drives rhizosphere bacterial community assembly during plant growth. *Soil Biol. Biochem.* **2015**, *85*, 170–182. [CrossRef]
66. Eisenlord, S.D.; Zak, D.R. Simulated atmospheric nitrogen deposition alters actinobacterial community composition in forest soils. *Soil Sci. Soc. Am. J.* **2010**, *74*, 1157–1166. [CrossRef]
67. Lee-Cruz, L.; Edwards, D.P.; Tripathi, B.M.; Adams, J.M. Impact of logging and forest conversion to oil palm plantations on soil bacterial communities in borneo. *Appl. Environ. Microbiol.* **2013**, *79*, 7290–7297. [CrossRef]
68. Siles, J.A.; Margesin, R. Abundance and diversity of bacterial, archaeal, and fungal communities along an altitudinal gradient in alpine forest soils: What are the driving factors? *Microb. Ecol.* **2016**, *72*, 207–220. [CrossRef]
69. Barka, E.A.; Vatsa, P.; Sanchez, L.; Gaveau-Vaillant, N.; Jacquard, C.; Klenk, H.P.; Clément, C.; Ouhdouch, Y.; van Wezel, G.P. Taxonomy, physiology, and natural products of Actinobacteria. *Microbiol Mol. Biol. R.* **2016**, *80*, 1–43. [CrossRef]
70. Natsuko, H.; Olson, S.H.; Ward, D.M.; Inskeep, W.P. Microbial population dynamics associated with crude-oil biodegradation in diverse soils. *Appl. Environ. Microbiol.* **2006**, *72*, 6316.
71. Kennedy, N.M.; Gleeson, D.E.; Connolly, J.; Clipson, N.J.W. Seasonal and management influences on bacterial community structure in an upland grassland soil. *FEMS Microbiol. Ecol.* **2005**, *53*, 329–337. [CrossRef] [PubMed]
72. Wang, K.; Zhang, Y.; Tang, Z.; Shuangguan, Z.; Chang, F.; Jia, F.; Chen, Y.; He, X.; Shi, W.; Deng, L. Effects of grassland afforestation on structure and function of soil bacterial and fungal communities. *Sci. Total Environ.* **2019**, *676*, 396–406. [CrossRef] [PubMed]
73. Landesman, W.J.; Nelson, D.M.; Fitzpatrick, M.C. Soil properties and tree species drive ß-diversity of soil bacterial communities. *Soil Biol. Biochem.* **2014**, *76*, 201–209. [CrossRef]
74. Zhou, J.; Guan, D.; Zhou, B.; Zhao, B.; Ma, M.; Qin, J.; Jiang, X.; Chen, S.; Cao, F.; Shen, D.; et al. Influence of 34-years of fertilization on bacterial communities in an intensively cultivated black soil in northeast China. *Soil Biol. Biochem.* **2015**, *90*, 42–51. [CrossRef]
75. Ren, C.; Wang, T.; Xu, Y.; Deng, J.; Zhao, F.; Yang, G.; Han, X.; Feng, Y.; Ren, G. Differential soil microbial community responses to the linkage of soil organic carbon fractions with respiration across land-use changes. *For. Ecol. Manag.* **2018**, *409*, 170–178. [CrossRef]
76. Gaiero, J.R.; McCall, C.A.; Thompson, K.A.; Day, N.J.; Best, A.S.; Dunfield, K.E. Inside the root microbiome: Bacterial root endophytes and plant growth promotion. *Am. J. Bot.* **2013**, *100*, 1738–1750. [CrossRef]
77. Jorquera, M.; Inostroza, N.; Lagos, L.; Barra, P.; Marileo, L.; Rilling, J.I.; Campos, D.C.; Crowley, D.E.; Richardson, A.E.; Mora, M.L. Bacterial community structure and detection of putative plant growth-promoting rhizobacteria associated with plants grown in Chilean agro-ecosystems and undisturbed ecosystems. *Biol. Fert. Soils* **2014**, *50*, 1141–1153. [CrossRef]
78. Davis, K.E.R.; Sangwan, P.; Janssen, P.H. Acidobacteria, Rubrobacteridae and Chloroflexi are abundant among very slow-growing and mini-colony-forming soil bacteria. *Environ. Microbiol.* **2011**, *13*, 798–805. [CrossRef]

79. Paul, E.A. *Soil Microbiology, Ecology, and Biochemistry*; Academic Press: Cambridge, MA, USA, 2015.
80. Trivedi, P.; Delgado-Baquerizo, M.; Anderson, I.C.; Singh, B.K. Response of soil properties and microbial communities to agriculture: Implications for primary productivity and soil health indicators. *Front. Plant Sci.* **2016**, *7*, 990. [CrossRef]
81. Filippidou, S.; Wunderlin, T.; Junier, T.; Jeanneret, N.; Dorador, C.; Molina, V.; Johnson, D.R.; Junier, P. A combination of extreme environmental conditions favor the prevalence of endospore-forming firmicutes. *Front. Microbiol.* **2016**, *7*, 1707. [CrossRef]
82. Veach, A.M.; Dodds, W.K.; Jumpponen, A. Woody plant encroachment, and its removal, impact bacterial and fungal communities across stream and terrestrial habitats in a tallgrass prairie ecosystem. *FEMS Microbiol. Ecol.* **2015**, *91*, fiv109. [CrossRef] [PubMed]
83. Lan, S.B.; Thomas, A.D.; Tooth, S.; Wu, L.; Elliott, D.R. Effects of vegetation on bacterial communities, carbon and nitrogen in dryland soil surfaces: Implications for shrub encroachment in the southwest Kalahari. *Sci. Total Environ.* **2021**, *764*, 142847. [CrossRef] [PubMed]
84. Põlme, S.; Bahram, M.; Jacquemyn, H.; Kennedy, P.; Kohout, P.; Moora, M.; Oja, J.; Öpik, M.; Pecoraro, L.; Tedersoo, L. Host preference and network properties in biotrophic plant–fungal associations. *New Phytol.* **2018**, *217*, 1230–1239. [CrossRef] [PubMed]
85. Merloti, L.F.; Mendes, L.W.; Pedrinho, A.; Souza, L.F.D.; Ferrari, B.M.; Tsai, S.M. Forest-to-agriculture conversion in Amazon drives soil microbial communities and N-cycle. *Soil Biol. Biochem.* **2019**, *137*, 107567. [CrossRef]
86. Nam, S.; Alday, J.G.; Kim, M.; Kim, H.; Kim, Y.; Park, T.; Lim, H.S.; Lee, B.Y.; Lee, Y.K.; Jung, J.Y. The relationships of present vegetation, bacteria, and soil properties with soil organic matter characteristics in moist acidic tundra in Alaska. *Sci. Total Environ.* **2021**, *772*, 145386. [CrossRef]
87. Rovira, P.; Vallejo, V.R. Labile, recalcitrant, and inert organic matter in Mediterranean forest soils. *Soil Biol. Biochem.* **2007**, *39*, 202–215. [CrossRef]
88. Qin, Z.; Yang, X.; Song, Z.; Peng, B.; Van Zwieten, L.; Yu, C.; Wu, S.; Mohammad, M.; Wang, H. Vertical distributions of organic carbon fractions under paddy and forest soils derived from black shales: Implications for potential of long-term carbon storage. *Catena* **2021**, *198*, 105056. [CrossRef]